Optical Engineering

SPIEDigitalLibrary.org/oe

Liquid-crystal photonic applications

Jeroen Beeckman
Kristiaan Neyts
Pieter J. M. Vanbrabant

Liquid-crystal photonic applications

Jeroen Beeckman
Kristiaan Neyts
Pieter J. M. Vanbrabant
Ghent University
Department of Electronics & Information Systems
Sint-Pietersnieuwstraat 41
Ghent, East-Flanders B-9000, Belgium
E-mail: Jeroen.Beeckman@elis.ugent.be

Abstract. Liquid crystals are nowadays widely used in all types of display applications. However their unique electro-optic properties also make them a suitable material for nondisplay applications. We will focus on the use of liquid crystals in different photonic components: optical filters and switches, beam-steering devices, spatial light modulators, integrated devices based on optical waveguiding, lasers, and optical nonlinear components. Both the basic operating principles as well as the recent state-of-the art are discussed.
[DOI: 10.1117/1.3565046]

Subject terms: liquid crystals; photonic applications; review; liquid-crystal lasers; spatial light modulators; tunable lenses; nematicons; optical nonlinearity.

Paper 100913SSR received Nov. 5, 2010; revised manuscript received Jan. 11, 2011; accepted for publication Jan. 13, 2011; published online Jun. 14, 2011.

1 Introduction

Liquid crystals (LCs) are organic materials that are liquid but that show a certain degree of ordering (positional and/or orientational). With this definition, many materials can be classified as liquid crystals, but the majority of liquid crystals that are used in photonic applications are of the thermotropic type. Thermotropic means that the liquid-crystal phase exists within a certain temperature interval (in contrast to lyotropic materials for which the material is liquid-crystal within a certain concentration range). Various types of thermotropic liquid-crystal materials exist, and many different mesophases have been discovered in the last decades: nematic, smectic A, smectic C, columnar, blue phases, and many many more. The diversity of liquid-crystal materials is huge, but this diversity is even overshadowed by the number of applications in which liquid crystals are used nowadays. The majority of applications are related to information-display applications. Liquid crystals have conquered the major market share in different display application areas: television screens, laptop screens, screens in mobile phones, etc. Only in projection displays does a tough competitor exist, namely microelectromechanical systems or licenced by Texas Instruments: Digital light processing. Organic light emitting diodes (OLEDs) are the obvious next generation technology that could overtake the LC domination, but today OLED displays have not penetrated the market and only the future will tell if they will. In this review article, we will focus on nondisplay applications, but because we cannot go too broad, we restrict ourselves to photonic applications in which the light is actively manipulated by the LC. In this review article, a certain external influence (surface anchoring, electric fields, optical fields) is used to (re)orient the LC in a certain way. In turn, the LC then changes the light that is propagating through it. Of course, as in every review article, it is impossible to list all the fascinating new scientific results or breakthroughs. Therefore, the authors apologize for not including some novel exciting phenomena or applications such as light-induced switching of LC polymers[1–3] or novel retardation structures such as broadband cholesteric filters.[4,5]

Numerous books and articles exist that deal with physical properties of LCs[6–8] and with display applications.[9–11] A very nice review on the different types of LC materials that exist for photonic applications is written by de Bougrenet de la Tocnaye.[12] In this review article, we will focus on the diversity of applications of LCs with special attention to the different configurations and engineering techniques that are applied.

2 Classification and Properties of Liquid Crystals

2.1 *Liquid Crystals: A Fourth Phase of Matter*

The liquid crystalline phase can be formed by different types of organic molecules. Anisotropy in either shape or solubility of the molecules is required. A balanced interaction between the molecules is the key to obtain a liquid crystalline behavior. In thermotropic liquid crystals, this interaction is in competition with the thermal motion of the molecules and the liquid-crystal phase is only stable within a certain temperature interval. Thermotropic liquid crystals usually have a high degree of anisotropy in the shape of the molecules (or mesogens). The most common type consists of rod-shaped molecules. The organic molecules typically have a long chain structure containing a side chain, multiple aromatic rings, and a terminal group on the other side.[13] As an illustration, Fig. 1 shows a 4-pentyl-4'-cyanobiphenyl molecule, which constitutes the well-known liquid crystal 5CB, which has been widely used in mixtures for display applications.

The 5CB molecule depicted in Fig. 1 has mirror plane symmetry and is therefore called achiral. The structure of chiral molecules is not planar but has different functional groups above and below the plane. Depending on the arrangement of the groups with respect to each other, two configurations (enantiomers) are possible. Enantiomers typically have identical chemical and physical properties, except for their optical activity.

2.2 *Nematic and Smectic Phases*

The ordering of thermotropic liquid-crystal molecules depends both on their chemical structure and temperature. For rodlike molecules, the ordering can be further classified as either nematic or smectic. The transitions from one mesophase to the other are reversible and occur at well-defined temperatures. The nematic phase of achiral liquid crystals can be

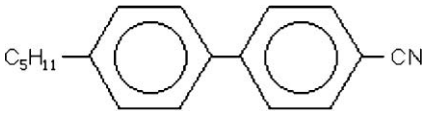

Fig. 1 Chemical structure of a 5CB molecule (4-pentyl-4'-cyanobiphenyl).

observed at temperatures below the clearing temperature for transition to the isotropic phase. In this case, the long-range orientational order dominates over thermal fluctuations and the molecules tend to align their long axes in a common direction (denoted by the director $\overline{L}$), as shown in Fig. 2(a). However, no long-range positional order of the molecules with respect to each other is present. The chiral nematic phase is very similar as for achiral mesogens, but the asymmetry of the molecules causes a gradual rotation of the director, which induces a spontaneous and continuous twist around the normal of the preferred molecular directions [Fig. 2(b)]. The distance over which the director has rotated over an angle 2π is called the pitch P_0 of the chiral nematic phase. If the temperature is decreased below the nematic range, then certain liquid crystals arrange in smectic layers. Depending on the molecular interaction energy, the smectic mesophase is typically further divided into the smectic A and smectic C phases. The molecules in the smectic A phase can freely rotate around the director, and the end group can point either up or down. In the smectic C phase, the molecules are arranged in smectic planes similar as in the smectic A phase. There is a higher order because the molecules are not able to rotate freely around their long axis and they are tilted with respect to the layer normal as indicated in Fig. 2(c). The end group of the molecules can still be oriented up or down.

2.3 *Properties of the Nematic Phase*

The mix of properties on the microscopic scale has lead to the excellent macroscopic electro-optic properties of liquid crystals, combining low viscosity (as in liquids) with anisotropy (typical for crystals). The nematic phase is most commonly used in applications because it is the easiest mesophase in terms of technology and in terms of understanding its behavior. The molecules are free to rotate around their long axis in the homogeneous nematic phase, yielding a full rotational symmetry. The symmetry elements of any physical property of a crystal must include the symmetry elements of the point group of the crystal (Neumann's principle[14]). This implies that homogeneous nematic liquid crystals have uniaxial macroscopic properties. Nematic liquid crystals exist with wide temperature range, different dielectric anisotropy ($-10 < \Delta\varepsilon < 20$), different birefringence ($0.07 < \Delta n < 0.5$) and high stability (mainly due to the development of fluorinated compounds).[15]

A certain orientation of the liquid-crystal layer in the relaxed state can be realized by using an appropriate alignment layer at the interfaces of the liquid crystal with the surrounding media. Even patterned alignment of the liquid crystal is possible by using photoaligned surfaces,[16,17] (e.g., for use in polarization gratings[18] or micropolarizers.[19]) The electrical properties of the nematic phase can be described by the 3×3 dielectric tensor, which takes the following form: $\varepsilon_{ij} = \varepsilon_\perp \delta_{ij} + \Delta\varepsilon L_i L_j$ (with $i, j = x, y, z$ and $\Delta\varepsilon = \varepsilon_\parallel - \varepsilon_\perp$). The orientation of the liquid crystal can be changed because of its dielectric anisotropy $\Delta\varepsilon$ by applying an external electric field $\overline{E}$. The corresponding energy density f_{electric} can be calculated as:[20]

$$f_{\text{electric}} = -\frac{1}{2}[\varepsilon_\perp |E|^2 + \Delta\varepsilon(\overline{L}\cdot\overline{E})^2]. \quad (1)$$

On the basis of this free energy, one can define a torque that acts on the liquid-crystal molecules due to the electric field. This torque is equal to $\bar{\Gamma} = \varepsilon_0 \Delta\varepsilon \left(\bar{L}.\bar{E}\right)\left(\bar{L}\times\bar{E}\right)$. The torque on the molecules is zero for an angle of 0 or 90 deg between the electric-field direction and the director axis. For an angle of 45 deg, the torque is maximal and, for a positive $\Delta\varepsilon$, the electric-field tries to align the director along the electric-field direction. Liquid-crystal molecules tend to reach an equilibrium state for which the free energy is minimized. If the applied voltage exceeds the Freedericksz threshold for elastic deformation, then the liquid-crystal tends to align parallel (as in case $\varepsilon_\parallel > \varepsilon_\perp$) or perpendicularly (as in case $\varepsilon_\parallel < \varepsilon_\perp$) to the electric field. Because of the optical anisotropy Δn, changing the orientation of the liquid-crystal also modifies the phase retardation for polarized light induced by the material. Such electrically controlled birefringence has been applied in the vast majority of liquid-crystal devices to date.

2.4 *Polymerization of Liquid Crystals*

In several applications, the liquid-crystal is stabilized by a polymer network by adding reactive compounds to the mixture. After exposure by UV light, the mixture with a photoinitiator is polymerized. In the polymerization reaction, the compounds are linked together and an anisotropic network is formed inside the liquid-crystal mixture, as shown in Fig. 3(a). The orientation of the liquid-crystal can still be changed electrically, but higher voltages are required because of the strong interaction between the liquid-crystal and

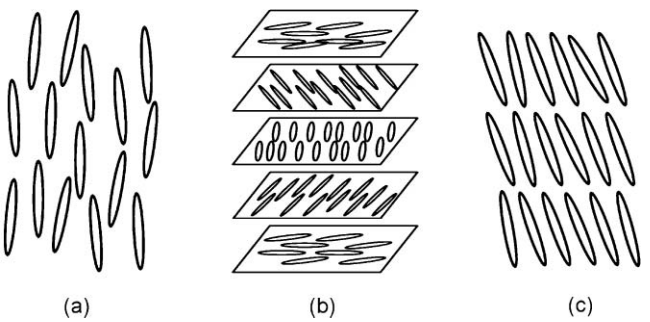

Fig. 2 Director configuration in (a) achiral nematic, (b) chiral nematic, and (c) smectic liquid-crystals.

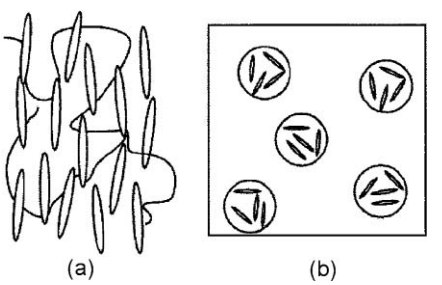

Fig. 3 Director configuration in (a) polymer stabilized and (b) polymer dispersed liquid-crystals.

the polymer network. When the electric field is removed, the liquid-crystal rapidly reaches the relaxed state because of the "memory effect" induced by the polymer network. When high polymer concentrations are used in the mixture, the liquid-crystal and polymer can become phase separated after polymerization. In this case, micrometer-sized droplets of liquid-crystal are embedded in a polymer matrix as shown in Fig. 3(b). Such polymer dispersed liquid-crystals (PDLCs) have been applied in switchable scattering devices. When no electric field is present, the liquid-crystal droplets are randomly oriented and a PDLC slab will scatter light because of the variations in refractive index. However, the liquid-crystal droplets can align in a common direction when an electric field is applied. Depending on the configuration, the system can act as a homogeneous transparant layer in case the refractive index of the polymer matches either the ordinary or extraordinary refractive index of the liquid-crystal.

2.5 *Blue Phases*

It has been observed that the helical structure of the chiral nematic phase [see Fig. 2(b)] of sufficiently low pitch cannot deform continuously on transition to the isotropic phase without the creation of defects.[21] As a result, an intermediate phase with a three-dimensional lattice of double-twist cilinders (in which the director rotates in a helical fashion about any axis perpendicular to a normal) occurs as shown in Fig. 4. Because the lattice constant is on the order of a few hundred nanometers, the structure can behave as a Bragg reflector in the visible part of the spectrum. In the original observation of this intermediate phase by Reinitzer, the material appeared as a blue substance because of Bragg reflection.[22] Hence, this interim phase was called the "blue phase". Blue phases are optically isotropic and have a high optical nonlinearity (Kerr effect, see Sec. 7.1), Thus, applying a sufficiently strong electric field induces birefringence in the liquid-crystal. Blue phases typically exist over a very narrow temperature range (∼1 K), which restricted their attractiveness for applications for a long time. However, blue phases stabilized over a wide temperature range (260–326 K in Ref. 23) have been demonstrated more recently, making them eligible to become the liquid-crystal phase of the future.

3 Filters and Switches

In display applications, the LC is used to modulate the light transmission through the different pixels. Crossed polarizers are used, and the liquid-crystal layer acts as a variable retarder to modulate the polarization of light passing through. In vertically aligned or in-plane-switching displays, a bright pixel is obtained by rotating the incoming polarization over 90 deg. This rotation is done by using the liquid-crystal layer as a half wave plate and thus engineering the optical retardation. In Twisted Nematic (TN) (or Super Twisted Nematic (STN)) displays, the situation is a bit more complicated because the retarder axis rotates. In order to make an optical filter or optical switch, one can use the same physical principles as the ones used in display applications. Here, we will focus on wavelength tunable filters, switches for optical signals in telecommunication, and tunable liquid-crystal lenses.

3.1 *Wavelength Tunable Filters*

In standard three-color imaging, one actually takes three images for three different colors or wavelength ranges. A color CCD, for example, often consists of RGB pixels in a Bayer arrangement, with double the amount of green pixels, compared to red and blue. In hyperspectral imaging, the aim is to obtain images of a certain object for much more different wavelengths and each image should be related to only a small wavelength range. The Lyot–Ohman tunable filter[24] was proposed in 1938, and today it is still the reference for hyperspectral imaging. These filters are commercially available, such as the VariSpec from Cambridge Research & Instrumentation (CRI). The principle of such a filter is best explained by considering Fig. 5. The device consists of a number of parallel polarizers with planar nematic liquid-crystal cells in between. The thickness of the liquid-crystal cells doubles with respect to the previous one: $d_{i+1} = 2.d_i = 2^i d_1$. The transmission of two polarizers in combination with one LC cell gives rise to the following transmission:

$$T = \frac{1}{2}\left(\cos\frac{\Gamma_i}{2}\right)^2 = \frac{1}{2}\left(\cos\frac{\pi\Delta n d_i}{\lambda}\right)^2. \tag{2}$$

By creating a stack of N steps, we obtain a transmission

$$T = \frac{1}{2}\prod_{i=1}^{N}\left(\cos\frac{2^{i-1}\Gamma_1}{2}\right)^2 = \frac{1}{2}\left[\frac{\sin(2^{N-1}\Gamma_1)}{2^N\sin(\Gamma_1/2)}\right]^2. \tag{3}$$

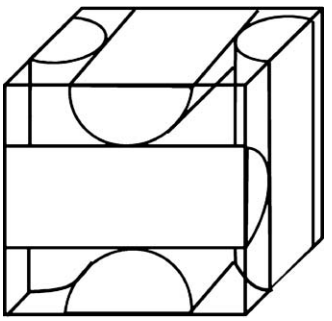

Fig. 4 Three-dimensional lattice of double helix cilinders in the blue phase.

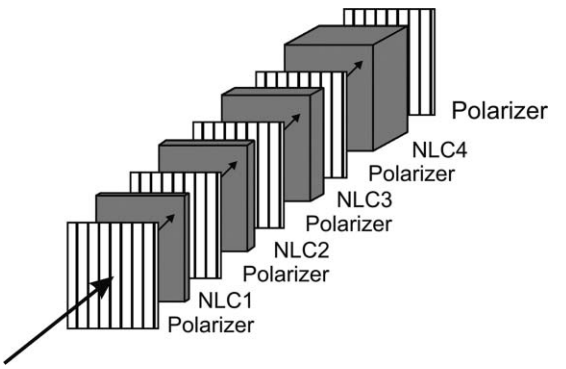

Fig. 5 Lyot–Ohman filter, which consists of a number of planarly oriented LC cells in-between parallel polarizers.

This results in a transmission spectrum with a central peak at a certain wavelength and a nearly zero transmission for other wavelengths. The width of the transmission peak decreases with increasing N, and also, the unwanted transmission at other wavelengths is suppressed. By changing the voltage applied to the different LC cells, the transmitted wavelength can be tuned. The thickest LC cell determines the speed of the device; thus, in practical devices, this thickness is minimized by combining the LC cell with a fixed retarder made, e.g., of quartz.

Even in the last few years there has been quite some work on Lyot-Ohman type devices because of the wide range of applications. Effort has been devoted to, e.g., sensing the different polarization properties of the incoming light,[25,26] polarization insensitivity,[27] or wider spectral ranges.[28–31]

The main drawback of these Lyot–Ohman filters is the high loss in transmission because of the series of polarizers. In any case, 50% of the light is lost because of the first polarizer. Additionally, practical polarizers only have a transmission of about 30–40% for unpolarized light.

Another class of tunable filters is based on the use of Holographic polymer dispersed liquid crystals. The liquid crystal is actually a mix of polymerizable material (typically, UV curing glue) and nematic LC. Interference of two UV laser beams, leading to a sinusoidal UV intensity, gives rise to polymer-rich regions and liquid-crystal rich regions in the cell in a periodic way. Writing a grating that is along the substrates leads to switchable diffractive gratings.[32] A grating with a period perpendicular to the substrates leads to a wavelength dependent filter with typically a reflection for a rather narrow wavelength band.[33,34] These gratings can be switched off by applying a voltage, providing that the refractive index of the polymer is matched with either $n_\perp$ or $n_\parallel$. The switching speed of these gratings are typically <1 ms.

3.2 *Optical Switches in Free Space*

Optical switches that switch light from one input fiber to a certain output fiber is not a simple task. Light in the fiber is caught in a high refractive index region and a set of high-precision lenses is necessary to couple the light coming out of one fiber into an output fiber with low losses. On top of that, it is necessary to perform switching with an electro-optic element with a certain speed and a minimum of cross talk. A very simple design for an $N \times N$ switch (*i.e.* with N inputs and N outputs) is shown in Fig. 6. Light from two input fibers goes to a matrix of 2×2 LC shutters by means of 50/50 splitters. The LC shutter either transmits or blocks the light. The light that passes through the shutter is then coupled into an output fiber. Again, a 50/50 splitter is necessary. In this way, an $N \times N$ switch can be fabricated with any arbitrary value of N, but in practice, this geometry is not usable because the losses are too high. First, for an $N \times N$ switch, only a factor $1/N^2$ of the light is coupled into the desired output. Additionally, 50% of the light is lost because the switch is usually polarization dependent.

A number of free-space switches have been presented in literature based on liquid crystals. There is nice, but outdated review by d'Alessandro and Asquini.[35] Different designs have been presented in order to reduce losses and cross talk and avoid the polarization dependency.[36–38] However, most of the promising free-space LC switches are based on

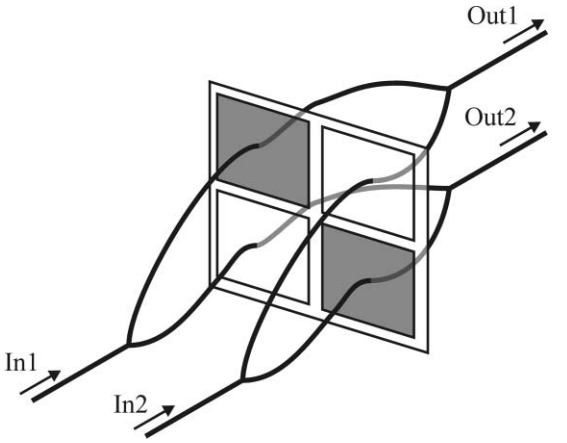

Fig. 6 Simple 2×2 optical fiber switch based on LC shutters.

a different principle, which is shown in Fig. 7. Light from an input fiber is projected onto a spatial light modulator (SLM) by means of a lens. The SLM changes the phase of the beam in a pixelated way after relection and in the Fourier plane of the lens, a certain intensity profile can be created by loading the correct phase pattern onto the SLM. By loading different phase patterns onto the SLM, the light can be coupled into one (or more) of the output fibers. These switches are actually based on holographic projection, and a number of devices have been demonstrated.[39,40] SLMs and their applications are discussed in more detail in Sec 4.

3.3 *Liquid-Crystal Lenses*

Lenses with an electrically tunable focal length and/or a repositionable focus are of broad interest for a number of applications. Because there are no moving parts in such a lens, they can be more reliable and able to withstand mechanical shock. Such tunable lenses can be applied in adaptive binocular glasses, autofocus cameras, LED light-steering applications,[41] 3-D confocal microscopy,[42] etc. A wide number of approaches have been studied to realize tunable lenses, and some of them are illustrated in Fig. 8. Figure 8(a) shows a configuration with a LC layer with nonuniform thickness. By using a liquid-crystal with $n_\perp < n_{\text{glass}} < n_\parallel$, it possible to tune the lens, going from concave to convex.[43] The biggest problem with LC is the fact that such lenses only work with one linear polarization component of the light so that a polarizer is necessary.

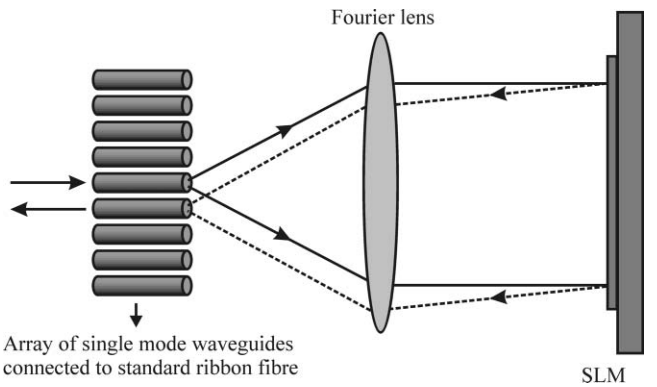

Fig. 7 Optical switch in freespace based on holographic projection.

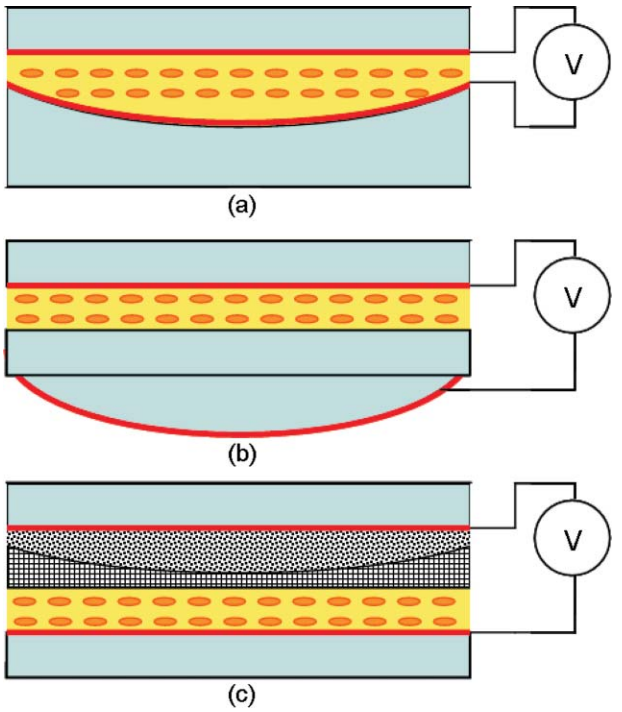

Fig. 8 Different approaches for tunable lenses with liquid-crystals.

Figure 8(b) shows a different approach in which the LC layer is homogeneous. Because of curvature of the glass and, hence, the nonuniform distance between the electrodes at a certain position in the cell, the LC switches inhomogeneously and thus results in a variable focal length.[44] Figure 8(c) shows a different approach that is nowadays succesfully used in autofocus cameras in cell phones.[45] The LC layer is again homogeneous, but due to the use of two different dielectric materials with different dielectric constants, the electric field in the LC layer is different at different positions. The refractive index of the dielectric materials are matched, so the LC layer itself fully incorporates the optical functionality, while the two dielectric materials take care of the electric functionality.

Two main other approaches have been studied extensively. One of the methods is to use a uniform LC layer, but to use a certain transparent electrode design to realize a spatially nonuniform electric field. The simplest approach is to pattern the transparent conductor in a way that a Fresnel-type lens is obtained with different zones of the liquid-crystal that are alternatively switched and not switched.[46] This approach however requires accurate fabrication of the electrode pattern. As an alternative approach, the combination of a weakly conductive layer in combination with a hole-patterned electrode can also produce a spatially dependent electric field across the LC layer. In literature often this approach is called a *modal-controlled* LC lens.[47–49] But it is difficult to obtain the correct electric field variation and to avoid aberrations with this method. A last method uses a uniform LC layer with uniform electrodes, and the nonuniformity of the LC switching is obtained by a gradient in the polymer concentration of a polymer stabilized liquid-crystal.[50,51]

4 Spatial Light Modulators

SLMs are versatile optical components that are used to manipulate the amplitude or phase pattern of a light beam in space. Liquid-crystal–based SLMs are very similar to (transmissive or reflective) liquid-crystal microdisplays: a matrix of electrically addressable pixels in which the orientation of the liquid-crystal is controlled by applying a voltage. Therefore, amplitude-modulating systems are very similar to projection systems: the pixels act as light valves for polarized light. As a result, the intensity profile of the light beam propagating through the SLM is modulated in space by the image imposed on the microdisplay. A phase-modulation setup consists of a transmissive or liquid-crystal-on-silicon microdisplay, which is operated without polarizers. Similarly, as in amplitude modulation systems, the liquid-crystal induces a variable phase-retardation per pixel to modulate the wavefront in space as shown in Fig. 9. In this section, we focus on two revolutionary applications of phase modulation with SLMs: laser-beam steering (an excellent overview can be found in Ref. 52) and holographic applications.

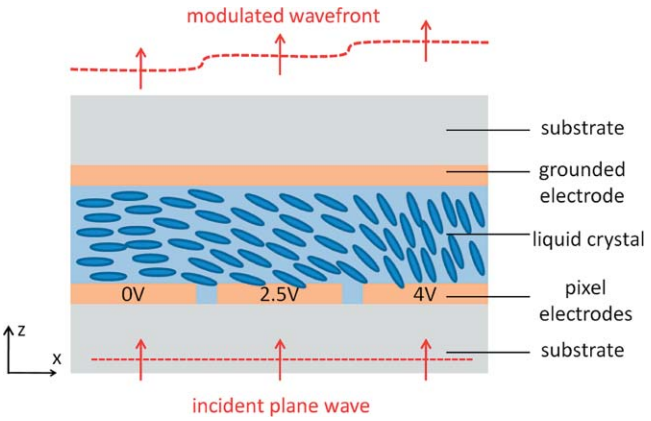

Fig. 9 Modulated wavefront of a plane wave polarized along the *x*-axis.

4.1 *Laser Beam Steering*

Shaping the phase retardation across the SLM allows nonmechanical beam steering similarly as in a prism or blazed grating: a linear phase retardation induces an optical path difference due to the difference in effective refractive index. As a result, the wavefront is tilted by this optical phased array[53] (OPA), and the beam is deflected to a nonzero angle. A sawtooth phase profile, as shown in Fig. 10 with abrupt 2π phase transitions (so-called flybacks) is used in devices (e.g., optical interconnects[54–56]) because this yields the same unfolded phase retardation for monochromatic light while limiting the maximum optical path difference to the wavelength λ. Continuous tuning of the beam deflection within a limited range can be realized[57] by either changing the period[58–60] or the blaze[61] of the phase profile.

In practice, mainly two factors limit the steering efficiency of liquid-crystal–phased arrays. The first limitation is associated to a nonideal 2π phase transition because the liquid-crystal deforms continuously. Furthermore, the voltage applied over the liquid-crystal changes abruptly between two neighboring pixels at the 2π phase transitions. However, the liquid-crystal orientation will be influenced by fringing electric fields between the pixels because the cell thickness is typically comparable to the pixel dimensions in search of high resolution.[62] As a result, the 2π phase transition is not only continuous because of the finite extent of the elastic

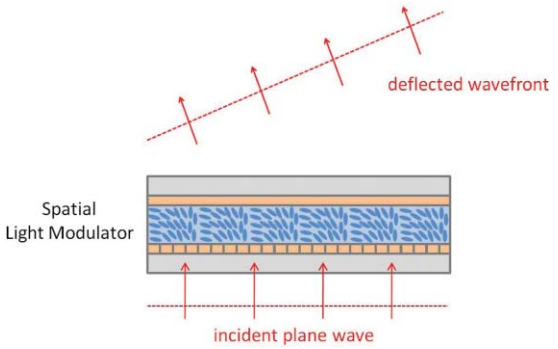

Fig. 10 Beam steering of a plane wave by a phased array.

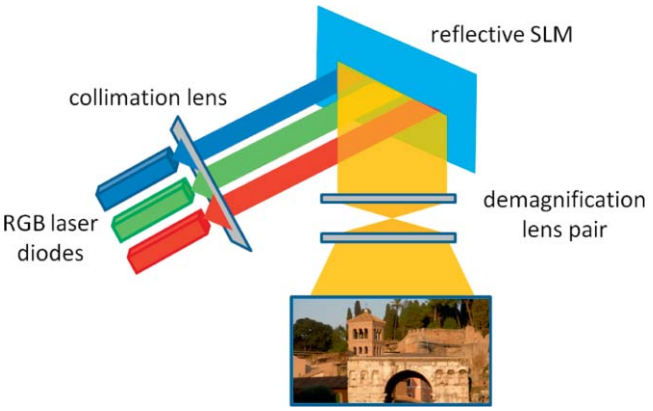

Fig. 11 Holographic projection setup.

deformation, but the flyback region is also elongated due to fringing fields.[63–65] The flyback region is the distance over which the 2π phase jump is smeared out. It has been shown that this effect is detrimental for the steering efficiency η at large angles θ.[58] If θ exceeds 5 deg (respectively, 10 deg), the efficiency is below 50%(respectively 25%), while no beam steering occurs ($\eta = 0$) if the desired deflection angle exceeds 20°.[52] Fringing fields can also induce undesired twisted regions in the director profile, which can induce depolarization.[63,66,67] A second limitation on the steering efficiency follows from the discretization of the phase profile because the driving voltage is constant per pixel in the phase array. This effect is however limited compared to the influence of fringing fields and can usually be neglected.[52] Further design considerations, such as the influence of surface alignment,[68] electrode configuration,[63] and silicon backplane,[69] have been described in the literature.

Because of their limited steering efficiency, liquid-crystal phased arrays are often used in combination with a second element capable of steering to discrete but larger angles.[70] Such a hybrid device can allow continuous steering over a wide angular range. Three classes based on liquid-crystals have been described in literature. A first approach is based on the spatial polarization separation induced by birefringent prisms.[71,72] A liquid-crystal OPA first deflects the beam under a small angle toward a cascade of birefringent prisms. Before each prism, the polarization state of the incident light is controlled by a tunable liquid-crystal layer. The light is refracted by each prism depending on its polarization state. The consecutive refractions steer the beam in the desired direction. An important drawback of such a system is that very thick (a few centimeter) prisms are required for wide-angle steering.[52] Instead of using birefringent prisms, a very similar system has been described that uses a cascade of thin liquid-crystal polarization gratings.[73] These gratings diffract light under wide angles at an efficiency that has been demonstrated to be close to unity over a wide range of grating periods and wavelengths.[74,75] In a third approach, a holographic medium is sandwiched between two liquid-crystal phased arrays.[76,77] The holographic medium[78] contains several fixed gratings for large-angle beam steering. The desired grating is addressed by the first phase array, and the second phase array adds continuous steering control over small angles to the wide-angle deflection of the grating.

4.2 *Holographic Applications*

Holographic systems are based on the inherent Fourier transform in the far field of a hologram illuminated by coherent light. Advanced algorithms exist in literature[79–83] to calculate a phase-only hologram image that yields the desired image in the far field. The resulting phase image can be generated by a SLM in which the liquid-crystal induces, per pixel, the desired phase. Therefore, SLMs can be used as reconfigurable diffractive optical elements for dynamic beam shaping,[84–86] correction,[87] and sampling.[88] This allows one to generate complex intensity profiles suited for laser material processing, such as dynamic photolithography.[89,90]

If the frame rate of the phase image is sufficiently high, then the SLM can be used as a holographic projector. To create a full-color video projector,[91] the phase-modulating SLM is time-sequentially illuminated by red, green, and blue laser diodes as shown in Fig. 11. A beam expanding lens pair can be used for providing wide projection angles in excess of 100 deg. The key to realize holographic projection systems lies in developing fast algorithms to calculate the phase images in real time.[92] The accurate calculation of these phase images still seems to be a limiting factor at the moment. Other real time applications include optical tweezers,[93] in which the position of the trapped particle can be manipulated by updating the hologram.

5 Waveguide-Based Devices

In the previous sections, liquid-crystal devices manipulate light beams that are traveling in free space. For display or camera applications, light in free space is inherently connected with the application. There are also many applications in which the propagation of light in free space is not essential, such as optical communication and optical sensing. For these applications, it can be useful to lock up the light in optical waveguides. In a waveguide, the diffraction of a light beam (which is always present in free space) is suppressed by the inhomogeneity of the optical medium. Typically, single-mode waveguides are used, in which (for one wavelength) only one mode can be transported, with a particular effective refractive index. Because liquid-crystals are easily influenced by an electric field or a temperature change (or by other effects), their presence near the core of the waveguide can be used to modify the effective refractive index of the light in the waveguide.

5.1 *Slab Waveguides*

A slab waveguide is a one-dimensional stack of homogeneous layers, where the light is confined in one (or more) layers of the stack. In the simplest form of isotropic materials, a central layer with the highest refractive index is sandwiched between two other materials with lower refractive indices. Depending on the thickness of the central layer (and on the refractive index contrast), one or more modes (TM or TE) can propagate in this one-dimensional structure. In a slab waveguide, with layers perpendicular to the x-axis, the light beam is confined in the x direction. This means that there is no diffraction in the x direction. There is no confinement in the yz plane, and a light beam propagating in the z direction with a limited beam width in the y direction will diffract and increase its width in the y direction. The effective refractive index of a mode in a slab waveguide depends on the refractive indices and the thicknesses of the layers in the stack.

If an anisotropic layer (for example, a liquid crystal) is placed on top of a slab waveguide, then the modes of the waveguide, their polarization, and their effective refractive index are modified, as schematically shown in Fig. 12. If the refractive index of the slab is much higher than the refractive index of the liquid-crystal (and if the slab is not extremely thin), then most of the light will remain in the slab and only a small evanescent part of the mode will propagate through the liquid-crystal. In this case, switching the orientation of the liquid-crystal will only have a small effect on the effective refractive index of the mode. If on the other hand, the refractive index of the LC is close to that of the slab or the slab is very thin, then the influence on the effective refractive index can be considerable.

Commercially, a number of components are already available that are based on slab waveguides covered with liquid-crystal. The liquid-crystal can be switched from planar to perpendicular to the plane of the waveguide by an applied voltage. Beacuse only the evanescent tail of the mode is influenced, a variation in the refractive index of 0.02 can be obtained by applying a voltage of 50 V over the LC.[94] This principle can be used to modulate the optical path difference between the fundamental TM and TE modes over ranges on the order of millimeters. Such large optical path differences can be used in broadband Fourier spectrometry for infrared detection of molecules.[94]

A light beam propagating (mainly) in the z direction in a slab waveguide can be modified by varying the optical path difference in the y direction. This can be done by varying the voltage along the y direction or by changing the length of the electrode as a function of the y coordinate. As a result, the phase will become a function of the y coordinate. This approach is similar to beam steering and modulation in free space. A linear variation of the phase delay with y will change the angle of the beam, and a parabolic variation of the phase delay will lead to a focusing or defocusing of the beam. This principle has also been used in Ref. 94.

When two slab waveguides are in each others vicinity, there can be coupling from one waveguide to the other if there is some overlap between the evanescent modes of both waveguides, as shown in Fig 12. The distance that the light must travel to transfer from one waveguide to the other is called the coupling length, which depends on the distance between the waveguides and on the refractive index of the material between them. If a layer of liquid-crystal is used as intermediate material, then the coupling length will depend on the orientation of the liquid-crystal. With an applied voltage, the orientation of the liquid-crystal and the coupling length can be modified. If the coupling section has a certain width, then the variation of the coupling length can be used to switch (or not switch) the light. This principle has been used by Clark and Hand shy[95] for realizing coupling between two slab waveguides, by using a thin layer of surface stabilized ferro-electric liquid-crystal. More detailed simulations for this system have been carried out by Ntogari et al.[96]

5.2 *Single Mode Integrated Waveguides*

The advances in the technology to make silicon devices is increasingly used to make two-dimensional single-mode photonic components. Depending on the material parameters (low or high index contrast) the dimensions of single-mode waveguides are of the order of (larger or smaller than) $1\mu m^2$. Such single-mode waveguides are made by high-resolution lithography.

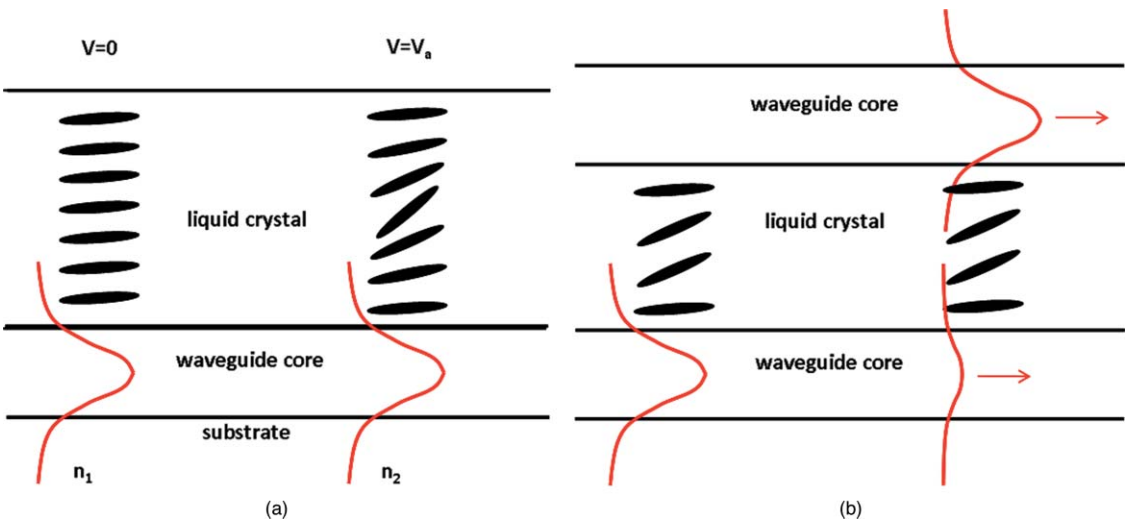

Fig. 12 Slab waveguides with liquid-crystal. (a) influence of the liquid-crystal on the effective refractive index and (b) switching from one slab waveguide to another by reorienting the liquid-crystal director

Because the dimensions of the single-mode waveguides are relatively small, there is an effect of the geometry on the orientation of the liquid-crystal. When the materials prefer parallel alignment of the liquid-crystal director, the director will try to align itself with sharp ridges in the surface. In this way, the director can be parallel to the two surfaces that are intersecting in the ridge. In this way, the structure of the layers influences the alignment.[97]

In the silicon-on-insulator(SOI) technology, there is a (high-index) silicon waveguide on a (low-index) silicon oxide slab. The silicon waveguide is single mode for the 1550-nm telecom band and has very low losses. In recent years, components such as ring resonators, Bragg gratings, wavelength-division multiplexers, and grating couplers have been produced with the SOI technology. Tuning of these devices is rather difficult because electro-optical effects in silicon are very small. Combining the SOI technology with electrically addressed liquid-crystals makes it possible to tune the wavelength of the photonic components over a relatively large range with a small voltage. A silicon-on-insulator ridge waveguide has a rectangular crosssection, with a thickness of 200 nm and a width on the order of 1 μm. In Ref. 98 the interferences in a Fabry–Perot cavity (formed by a straight waveguide between two facets of the silicon) shift over 0.3 nm under influence of an applied ac voltage (10 V) over the liquid-crystal.

Several groups have investigated the properties of SOI microring resonators, covered by liquid-crystal. In the work of Maune, the electric field is parallel with the plane of the ring resonator. Here, a shift of 0.22 nm in the resonance frequency for TE polarized light was obtained for a voltage of 10 V. The experimental finding by De Cort et al. of a 0.5-nm shift for an electric field perpendicular to the ring-resonator plane was confirmed by numerical simulations.[99] A similar ring-resonator structure has been patented by Chigrinov et al.[100] Numerical FDTD simulations of SOI waveguides with LC predict a shift in the resonance wavelength for TM polarized light up to 38 nm.[101]

There is also work on waveguides that do not use silicon as the core material. Silicon nitride with refractive index 1.67 can also be used for the core of the waveguide. The refractive index contrast with the substrate and the liquid-crystal is then smaller, and the waveguides have a width of 3 μm.[102] In this paper, the waveguide contains a section with two modes (symmetric and antisymmetric) that propagate at different speeds. By switching the orientation of the LC overlay, the two speeds are modified and the interference between the two modes can be used to switch the light into one of two exit ports. The waveguide core can be omitted altogether, when the waveguide is formed by the liquid-crystal alone. The principle of switching between two exit ports by using a waveguide section with two modes has been demonstrated in Ref. 103. In the experiments of d'Alessandro et al.[104], V-grooves in silicon (covered with an oxide) are filled with liquid-crystal, which can be switched under influence of a voltage.

6 Lasing

In order to achieve lasing, there are basically two requirements. First, there must be a section in the device where there is gain of light propagating through it. Second, there must be a way to keep the light that is generated inside some kind of cavity, so that the light that is generated remains in the cavity for a sufficient time. This can be achieved, for example, by putting two mirrors at both sides of the gain medium. If the optical fields in the gain medium become large enough then stimulated emission can be achieved.

The role of liquid-crystals for lasing applications is twofold. First, liquid-crystal can be used as a way to tune the cavity length of an existing laser. Second, liquid-crystal can play the role of gain medium and cavity at the same time.

6.1 *Tuning Lasers with Liquid-Crystals*

The wavelength at which one will obtain lasing is defined by the fact that one round-trip of the light through the cavity must result in a phase difference of $2m\pi$, with m an integer. Suppose that the cavity length is d and that the cavity is filled with a material with refractive index n, the requirement for the wavelength is $\lambda = 2nd/m$. A liquid-crystal device can be incorporated inside the cavity of an existing laser, as shown in Fig. 13. By changing the orientation of the liquid-crystal, one changes the effective cavity length of the laser (by changing the refractive index of the liquid-crystal medium). In this way the emission wavelength can be tuned, as long as the gain medium has a gain spectrum that extends over the desired wavelength range. This principle was demonstrated in Refs. 105 and 106 for the tuning of semiconductor lasers and in Ref. 107 by putting the liquid-crystal on top of a vertical cavity surface emitting laser.

Another way to tune the lasing characteristics is not to use the LC device as a variable retarder, but as a filter or switching element. Changing the transmission of the LC device for different wavelengths will promote lasing for certain wavelengths and increase losses for other wavelengths. In this way, one can force the laser to lase at a certain wavelength and different techniques have been reported in literature: by using a LC tunable mirror,[108] by using the LC device as a deflector in combination with a grating[109] and by using a photonic crystal fiber filled with LC.[110]

6.2 *Liquid–Crystal Lasers*

Chiral nematic liquid-crystals exhibit a uniform twisting of the director along a certain direction, as shown in Fig. 14(a). Because of the periodicity of the structure, there is a periodic modulation of the refractive index and a one-dimensional photonic stop band is created. Circularly polarized light with either right or left handedness and with a wavelength that is

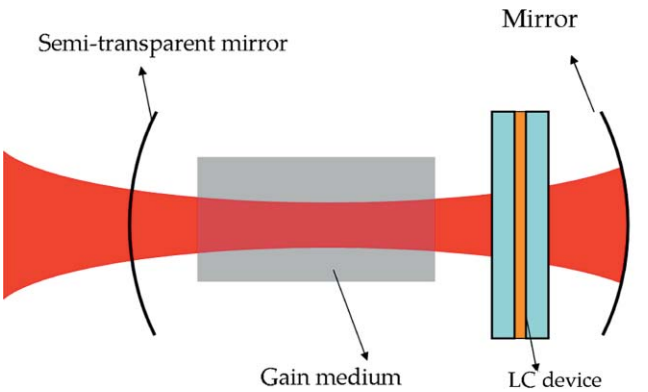

Fig. 13 Gain medium in a cavity formed by two mirrors leads to lasing. A liquid-crystal device in the cavity can be used to tune the lasing characteristics.

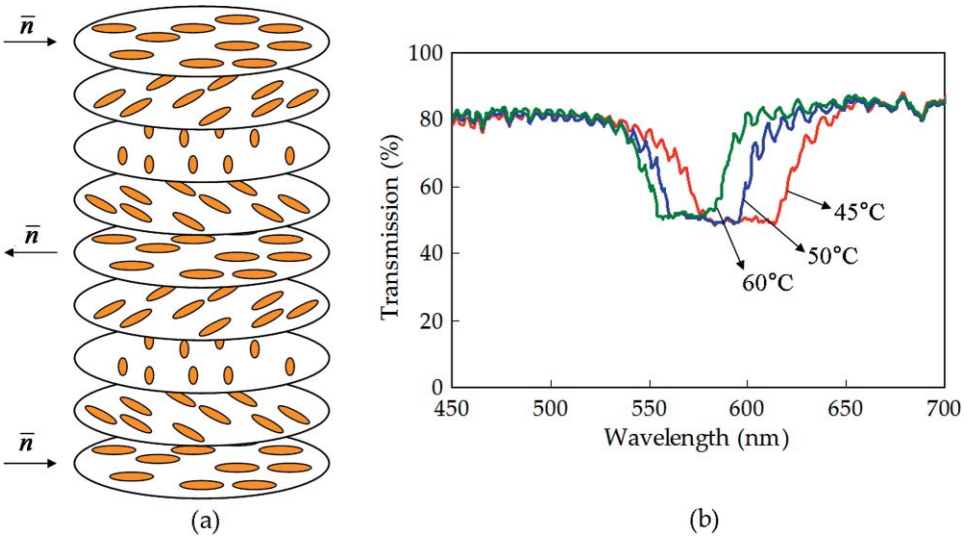

Fig. 14 (a) Transmission spectrum of a typical chiral LC cell. (b) One pitch of a chiral nematic liquid-crystal is shown along the vertical direction is shown.

situated in the stop band is reflected, the other handedness is not reflected, which gives rise to the transmission spectrum in Fig. 14(b). This spectrum is recorded for a mixture of 54% Cholesterylpelargonate (chiral LC) and 46% E7 (nematic LC from Merck). The center wavelength λ_c of the stop band is determined by the pitch P and the average refractive index n of the LC as $\lambda_c = nP$. Changing the temperature leads to a change in pitch, and this provides a simple way to visualize temperature changes as the color of the reflected light changes.

When light is generated inside the liquid-crystal with a wavelength in the stop band, it is difficult for the light to exit the cell along the direction of the pitch (at least for one circularly polarized component). This gives rise to a resonance process for the light, similar to distributed feedback (DFB) lasers. The generation of light is typically achieved by mixing organic dyes in the LC. With this principle, the first demonstration of laser-light generation in dye-doped LCs was reported by Ilchishin et al.[111] in 1980. Two review articles give a very nice overview of the work that has been carried out in the last three decades on lasing in LC material.[112,113] This section only presents a very brief overview of the most important results. In most of the reported works on LC lasers, band-edge lasers are investigated. This means that lasing occurs at one of the two edges of the stop band, as in Fig. 14(b), and the side with the longest wavelength offers the lowest threshold. The fact that the lasing occurs preferentially at the edge and not in the center of the stop band can be explained in two ways. The first way is best understood by making an analogy with the bandgap in semiconductor materials. In the bandgap, no electrons can exist because the density of states is zero. Most of the electrons are located near the edges of the bandgap because the density of states is higher and because of the Boltzman (actually, Fermi) statistics. For the LC laser, it is similar: the highest density of states for the photonics is located near the edges of the photonic stop band and thus leads to a preferential wavelength for laser emission. Another way to understand this phenomenon is to consider the theory for DFB lasers. A DFB laser consists of a periodic grating, but in order to reduce the threshold drastically, it is required to include a defect with a $\lambda/4$ shift in order to fulfill the phase conditions. Introducing this defect leads to lasing in the middle of the photonic bandgap; without this defect, lasing occurs at a much higher threshold at the edges of the bandgap. The latter is exactly what is happening in chiral LC lasers.

Typically, a pulsed pump laser is used, which is injected under a certain angle with the substrates. Laser light is generated along the helical pitch (*i.e.* perpendicular to the substrates). The most important advantage of chiral LC lasers is the possibility of tuning the laser wavelength. One obvious way to is change the temperature of the LC cell, which affects the pitch and thus the position of the photonic stop band.[114] By using a blend of several different dyes with a different emission spectrum, a wide spectral range can be covered,[115] only limited by the wavelength of the pump laser, which dictates the lowest possible wavelength. A big obstacle for applications is the fact that pulsed lasers are necessary for the laser action, and a large effort is spent to reduce the necessary thresholds for lasing. Pumping with blue LEDs has been reported, but there is still a long way to go to achieve CW lasing.

Apart from temperature tuning of the wavelength, several other mechanisms have been reported. Doping the LC mixture with photoactive agents and illumination with UV radiation may lead to a change in pitch length and thus a change in wavelength.[116,117] Voltage tuning may seem to be an easy way, but it is not because an applied voltage will cause a distortion of the helical structure and thus will prevent lasing.[118] Therefore, one must resort to certain tricks to achieve voltage tuning, such as negative dielectric chiral materials[119] or by using smectic LC.[120]

Two other classes of liquid-crystal lasers can be identified in which there is no intrinsic chirality or periodicity in the liquid-crystal. In random lasers, the random scattering of the light in nematic liquid-crystals offers enough optical feedback to start lasing, as demonstrated in a thick nematic cell of 100 μm thickness[121] and in a freely suspended film of liquid-crystal.[122] Another way to provide the periodicity is to make holographic gratings in polymer-dispersed liquid-

crystals. The grating can then be switched on and off by applying a voltage and thus also the lasing.[123]

7 Optical Nonlinearity: Spatial Solitons

When illuminating a material with a beam of a certain shape and intensity, one expects that the same beam with the double intensity will result in the same beam coming out the materials but with the double intensity. This is the linear situation. A simple example of a nonlinear situation is the effect of second harmonic generation (SHG). At low optical power, the outcoming beam will have the same wavelength as the incoming beam. At high powers however, the outcoming beam will have a different wavelength, namely, half the wavelength (or twice the frequency). Similar kinds of nonlinearities are nowadays widely used in laser systems to generate light with a particular wavelength. Backed by the commercial importance, the study of optical nonlinearities has become a large scientific field in optics.

7.1 *Nonlinear Effects*

The same optical nonlinear effects in liquid-crystals exist as in conventional materials, but many liquid-crystal–specific nonlinearities exists that do not appear in other materials. A very nice overview can be found in the works of Khoo[7,124] and Simoni,[125] and in this review article, we will try to give a basic overview.

7.1.1 *Electronic Nonlinearities*

The general relation between the electric displacement and the electric field can be written as $\bar{D} = \varepsilon_0 \bar{E} + \bar{P}$. The polarization $\bar{P}$ arises from the fact that the electrons in the atoms react to the fields of the electromagnetic wave. For a linear isotropic material;

$$\bar{D} = \varepsilon_0 \bar{E} + \varepsilon_0 \chi_L \bar{E} = \varepsilon_0 \varepsilon \bar{E} \tag{4}$$

Roughly speaking, this is the case when the displacement of the electrons reacts in a linear way to the force from the optical electric field. For nonlinear materials, we can write the total polarization as a sum of the linear polarization and the nonlinear polarization $\bar{P} = \varepsilon_0 \chi_L \bar{E} + \bar{P}_{NL}$. The polarization is often expanded as a power series in $\bar{E}$, and in general, it can be written as:

$$P_i = \varepsilon_0 \chi_{ij}^{(1)} E_j + \varepsilon_0 \chi_{ijk}^{(2)} E_j E_k + \varepsilon_0 \chi_{ijkl}^{(3)} E_j E_k E_l + \cdots \tag{5}$$

In Eq. (5), the susceptibility with index (1) is of course the linear susceptibility and the rest are higher order susceptibilities responsible for the nonlinear effects. Starting from Maxwell's equations, we can then find the wave equation for nonlinear media;

$$\nabla^2 \bar{E} - \varepsilon_0 \varepsilon \mu_0 \frac{\partial^2 \bar{E}}{\partial t^2} = \mu_0 \frac{\partial^2 \bar{P}_{NL}}{\partial t^2} \tag{6}$$

Susceptibilities of orders higher than 2 or 3 are hardly ever used. The light powers that are needed to generate nonlinearities with $\chi^{(2)}$ or $\chi^{(3)}$ are already very high so that often only pulsed lasers can generate an intensity that is large enough. In the following subsections, two very well-known effects are described that use either the $\chi^{(2)}$ or the $\chi^{(3)}$ nonlinearity.

Second harmonic generation $\chi^{(2)}$. SHG occurs in materials with a nonzero $\chi^{(2)}$. If we assume that the optical fields are scalar and can be written as $E = A\cos[\omega t - k(\omega)z]$, then the nonlinear polarization can be written as:

$$\begin{aligned} P_{NL} &= \varepsilon_0 \chi^{(2)} A^2 \cos^2[\omega t - k(\omega)z] \\ &= \varepsilon_0 \chi^{(2)} \frac{A^2}{2} \cos[2\omega t - 2k(\omega)z] + \varepsilon_0 \chi^{(2)} \frac{A^2}{2}. \end{aligned} \tag{7}$$

From Eq. (7) we can see that there are actually two source terms for the generation of electric fields with different frequencies than ω. There is a term with the double frequency 2ω and one with zero frequency. The first one is of course the one that is responsible for the SHG. To generate light with the double frequency with an acceptable efficiency, it is required to have phase matching, but this will lead us too far, thus we refer the reader to one of the numerous books on optical nonlinearity. Only noncentrosymmetric materials have a nonzero $\chi^{(2)}$, which means that SHG does not occur in nematic LC, except at the surfaces where the molecules can be ordered in a polar way.[126] Various smectic phases are noncentrosymmetric and allow for a very high $\chi^{(2)}$ coefficient.[127]

Kerr nonlinearity $\chi^{(3)}$. The Kerr effect occurs in media that have a nonzero $\chi^{(3)}$. If the nonlinear polarization has the form $P_{NL} = \varepsilon_0 \chi^{(3)} E^3$, then we can write

$$\begin{aligned} P_{NL} &= \varepsilon_0 \chi^{(3)} A^3 \cos^3[\omega t - k(\omega)z] = \varepsilon_0 \chi^{(3)} A^3 \\ &\quad \times \left\{ \frac{3}{4} \cos[\omega t - k(\omega)z] + \frac{1}{4} \cos[3\omega t - 3k(\omega)z] \right\}. \end{aligned} \tag{8}$$

We can see that two frequencies are generated: ω and 3ω. For the Kerr effect, the frequency 3ω is of no importance; thus, we neglect this component and rewrite the total polarization as $P = \varepsilon_0 \left[\chi^{(1)} + \frac{3}{4}\chi^{(3)} A^2\right] E$. From this equation it is clear that we can define a *new* susceptibility $\chi' = \chi^{(1)} + \frac{3}{4}\chi^{(3)} A^2$ and subsequently also a new refractive index

$$\begin{aligned} n' &= \sqrt{1 + \chi'} = \sqrt{n_0^2 + \frac{3}{4}\chi^{(3)} A^2} \\ &\approx n_0 + \frac{3}{8n_0}\chi^{(3)} |E|^2 = n_0 + \frac{3\chi^{(3)}}{8n_0^2 \varepsilon_0 c} I \end{aligned} \tag{9}$$

$$n' = n_0 + n_2 I. \tag{10}$$

This new refractive index is dependent on the intensity of the light and describes the nonlinear optical Kerr effect. This is a nonlinearity that can simply be described by an index of refraction that is linearly dependent on the intensity of the light, and n_2 can be either positive or negative. The value for n_2 in fused silica used in optical fibers, is positive and $\sim 3\times10^{-16}\,\mathrm{cm}^2/\mathrm{W}$.[128] Let us make a simple calculation to illustrate this value. To achieve an index change of 10^{-6} in an optical fiber where the light is confined in a circular region of 4 μm diam, an optical power of $\sim$2.5 kW is needed. These are values that can only be achieved with pulsed lasers. The liquid CS_2 has an n_2 coefficient, which is much higher $3\times10^{-14}\mathrm{cm}^2/\mathrm{W}$, but still the required powers are very high and hardly achievable with continuous-wave lasers.

7.1.2 *Thermal and Density Effects*

Basically, three mechanisms can be distinguished when we speak about thermal nonlinearity: density effects due to

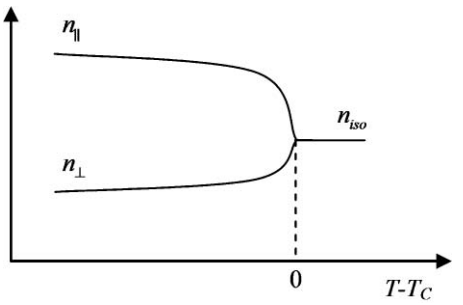

Fig. 15 Evolution of the refractive indices of a nematic liquid-crystal in function of the temperature.

electrostriction, density effect due to heating, and changes in the order-parameter due to heating. But only the last phenomenon is specific to LCs, which is the reason why we restrict ourselves to this effect.

The order parameter of a liquid-crystal is a way to express how well the individual molecules in the liquid-crystal are aligned. An order parameter equal to 1 means that all molecules are perfectly aligned along one direction. A value of zero means that the molecules are randomly oriented and the material is thus macroscopically isotropic. Typical nematic liquid-crystals have an order parameter of 0.4–0.7, and this value drops to zero when reaching the clearing temperature (i.e., the temperature at which the liquid-crystal becomes an isotropic fluid). Figure 15 shows the evolution of the refractive indices as a function of the temperature, and the variation in refractive index is mainly due to order-parameter variations. When launching a laser beam in the liquid-crystal, the material heats. For a polarization parallel to the director, the refractive index will decrease, Whereas a polarization perpendicular to the director will see an increase in refractive index. This corresponds to respectively a self-defocusing and a self-focusing nonlinearity.

7.1.3 *Reorientational Nonlinearity*

Similar to the reorientation of the director by a static electric field (as explained in Sec. 2.3), it is also possible to reorient the director by an optical electric field. The same equations for the static situation are valid here. Because the complex notation for the optical fields are often used in wave propagation, we account for the possibility of having complex field components and, therefore, in the next formulas $\bar{E}^*$ will appear, which means that we take the complex conjugate of $\bar{E}$. The optical energy per volume unit can be written as

$$\begin{aligned} F^{\mathrm{o}} &= -\frac{1}{2}\bar{D}^*.\bar{E} = -\frac{\varepsilon_0}{2}\bar{E}^*.\bar{\bar{\varepsilon}}.\bar{E} \\ &= -\frac{\varepsilon_0}{2}E_i^*(\varepsilon_\perp\delta_{ij} + \Delta\varepsilon L_i L_j)E_j \\ &= -\frac{\varepsilon_0\varepsilon_\perp}{2}(\bar{E}^*.\bar{E}) - \frac{\varepsilon_0\Delta\varepsilon}{2}(\bar{L}.\bar{E}^*)(\bar{L}.\bar{E}) \\ &= -\frac{\varepsilon_0\varepsilon_\perp}{2}|\bar{E}|^2 - \frac{\varepsilon_0\Delta\varepsilon}{2}|\bar{L}.\bar{E}|^2. \end{aligned} \tag{11}$$

Only the last term that contains the director orientation is important for the calculation of the director orientation. Suppose that the orientation of the electric field and the director make an angle $\pi/2-\theta$, then this energy can be written as

$$F^{\mathrm{o}} = -\frac{\varepsilon_0\Delta\varepsilon}{2}\sin^2\theta|\bar{E}|^2, \tag{12}$$

and the torque has the following value

$$\Gamma^{\mathrm{o}} = \varepsilon_0\Delta\varepsilon\sin\theta\cos\theta|\bar{E}|^2. \tag{13}$$

This torque tries to rotate the molecules so that they are aligned along the electric field. Equation (13) shows that the reorientation is only dependent on the squared amplitude of the electric field. The sign of the electric field does not play a role. Thus, for the calculation, it is similar whether we work with dc fields, ac fields, or optical fields; only the values for $\Delta\varepsilon$ should be adapted according to the frequency of the electric field. This nonlinearity is huge compared to typical electronic nonlinearities with an equivalent Kerr coefficient on the order of 10^{-3} cm^2/W. Typical Kerr coefficients for glass are in the order of 10^{-16} cm^2/W.

Next to the reorientation effect in the nematic phase, reorientation also occurs in the isotropic phase, but the nonlinearity is several order of magnitude smaller than the reorientation in the nematic phase. In the isotropic phase, the liquid-crystal molecules are randomly oriented but tend to align their highest polarizability tensor component along the optical electric field, which results in some degree of preferred orientation. Also, in conventional liquids, this reorientation effect occurs. The best example is the widely used fluid CS_2 in nonlinear optics, which has an equivalent n_2 nonlinear coefficient of 3×10^{-14} cm^2/W. However, in the isotropic phase of the liquid-crystal, there are molecular correlations but, because the temperature is too high, no ordering appears. However, these molecular interactions help to increase the nonlinearity and the nonlinear coefficient near the clearing temperature varies as $1/(T-T^*)$. For 6CB for example, a nonlinear coefficient $n_2 \approx 6\times10^{-13}$ cm^2/W was found,[129] which is more than one order higher than the value for CS_2. The drawback is that the response time of this effect is in the order of 10 ns instead of a few picoseconds.

7.1.4 *Dye Enhanced Nonlinearity*

During the last two decades, different photosensitive dyes or molecular dopants have been added to the liquid-crystal material in order to enhance the nonlinearity. The different authors of articles on this topic have surpassed one another, not only in the reported nonlinear coefficients (ranging from 10^{-3} to 1000 cm^2/W), but even more in the superlatives that were used to describe the value this coefficient (ranging from giant, huge, ..., all the way to colossal. One of the common ways to enhance the nonlinearity is to dope the liquid-crystal with the dye methyl-red. The way that the increase in nonlinearity is explained is that the reorientational torque of the optical electric field is enhanced by the dye, as explained in the paper of Janossy.[130] But the exact physical mechanism was, a few years ago, still a topic of debate, and the role of the surfaces of the LC cell might be an important factor in the mechanism.[131,132]

Another way to obtain very high nonlinearity—for which the mechanism is quite well understood—is to use azobenzene LC. The LC molecules is similar to regular nematic LC molecules, such as 5CB, but they contain an azobenzene group (see Fig. 16). The azobenzene group undergoes trans-cis isomerization under influence of light and temperature. In

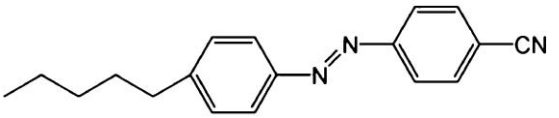

Fig. 16 Azobenzene nematic liquid-crystal with a very similar structure as 5CB.

the trans state, the material is nematic because the molecule has an elongated shape. From a certain concentration of cis-state molecules, the material loses its liquid-crystalline properties and becomes isotropic. It is clear that the influence of the trans-cis isomerization on the order parameter (and hence also the refractive index) is a strong effect that can even happen in quite fast time scales (on the order of nanoseconds[133]).

7.2 *Two-Beam Coupling*

If we consider a light beam propagating with an angle ϕ with respect to the z-axis, then electric field can be described by $\bar{E}(x,z) = \bar{E}_0 \exp(-j\bar{k}.\bar{r})$ with $\bar{k} = k_0(\cos\phi\,\bar{1}_z + \sin\phi\,\bar{1}_x)$. Suppose that another beam propagates with an angle $-\phi$ with respect to the z-axis with the same linear polarization as the other beam. Then, if both beams coincide at position $z = 0$, a sinusoidal variation occurs in the beam amplitude at this position: $2\bar{E}(x,0) = \bar{E}_0 \cos(k_x x)$, with $k_x = k_0 \sin\phi$. The period of the amplitude modulation is given by $\lambda/\sin\phi$ and the period of the intensity modulation by $\lambda/2\sin\phi$. If the medium that is present at $z = 0$ is linear and uniform, then further propagation of the two beams is unaffected and two spots are visible in the diffraction pattern. Suppose that the medium is uniform but nonlinear, then the refractive index in the $z = 0$ plane is modulated in a periodic way. This modulation leads to additional diffraction spots. In literature different authors use different names for this effect, such as photorefractive two-beam coupling or holographic grating formation, but in principle, the underlying physics is the same. This nonlinear effect has a variety of applications, ranging from data storage, hologram recording, and optical interconnections to beam combining.

The research field is very active, and again, it is impossible to give a full overview in this review article. In pure nematic liquid-crystals the nonlinearity is rather small and quite high laser powers are necessary.[134] Quite a great deal of effort is spent in order to increase the nonlinear coefficient and to reduce the necessary optical powers. Pure nematic LC in combination with a layer of photoconductive material can be used,[135] fullerene C60-doped liquid-crystals,[136,137] dye doped liquid-crystals[138,139] and in the last few years, quite a lot of attention went to the use of ferroelectric nanoparticles in order to improve nonlinearity.[140]

7.3 *Solitons*

Solitary waves have been the subject of intense studies in many fields, including hydrodynamics, nonlinear optics, plasma physics, etc. Historically, it is assumed that the first solitary wave was reported by James Scott Russell in 1844. He observed a wave in a narrow channel of water that propagated fast along the channel and the original shape of this wave did not change along the propagation. Only after a long distance did the wave disappear. It was in the 1960s that the term "soliton" was proposed because of the particlelike nature of these solitary waves. Indeed, after collision with each other, these solitary waves remained intact. In optics, it is common to use the two terms as synonyms, although this is not completely correct. For a good overview on optical solitons, refer to Refs. 141 and 142.

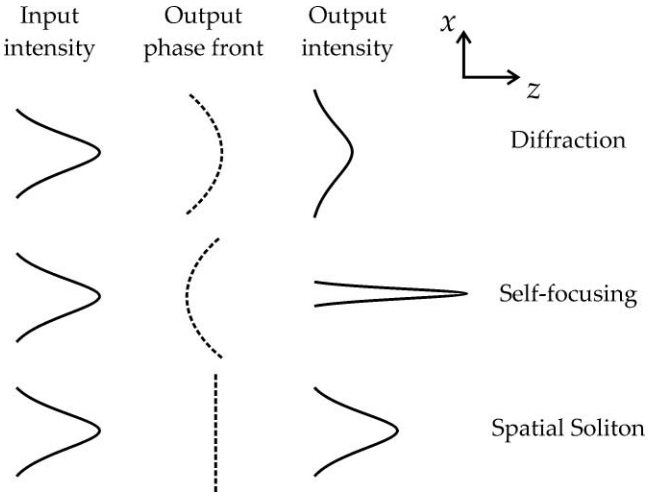

Fig. 17 Schematic illustration of the lens analogy for spatial solitons.

To understand the generation of spatial solitons, one should keep in mind that every optical beam of finite size diffracts in a uniform medium. Consider Fig. 17 for a better understanding. A diffracting beam after some propagation distance will be smeared out, the maximum intensity drops down, and the width increases. Diffraction thus acts as a concave lens, because the output phase front will have also changed as it passed through a concave lens. This diffraction can be counteracted when the medium has a higher index of refraction near the center of the beam. This higher index of refraction can be due to a nonlinear self-focusing effect, such as the Kerr nonlinearity. This nonlinear effect thus acts as a convex lens, and the beam width will narrow. When the two effects are balanced and the phase front of the beam remains plane, the beam will propagate without change in shape or intensity and a spatial optical soliton is formed.

In essence, this means that the beam creates its own waveguide and the beam is a spatial soliton when it is a mode of its own induced waveguide.[143] In this way, we can also call a spatial soliton a self-induced waveguide. This induced waveguide is in turn, able to guide a second low-power probe beam. It is thus a real waveguide. The only difference is the origin and the fact that it disappears when the light disappears.

Spatial solitons in nematic liquid-crystals are often referred to as "nematicons" as first proposed by Assanto et al.[144] The generation of nematicons has been demonstrated with different types of optical nonlinearities: reorientational, thermal and azobenzene LC nonlinearity.

The reorientational nonlinearity in LCs is always of the self-focusing type, and some of the first results on soliton generation with this effect have been demonstrated by Karpierz et al.[145] and Peccianti et al.[146] after which many publications were devoted to further investigation of the soliton-generation mechanism.[145,147–153] One of the easiest configurations to understand, the soliton generation is the configuration for which the liquid-crystal is aligned uniformly, making an angle of 45 deg with respect to both the

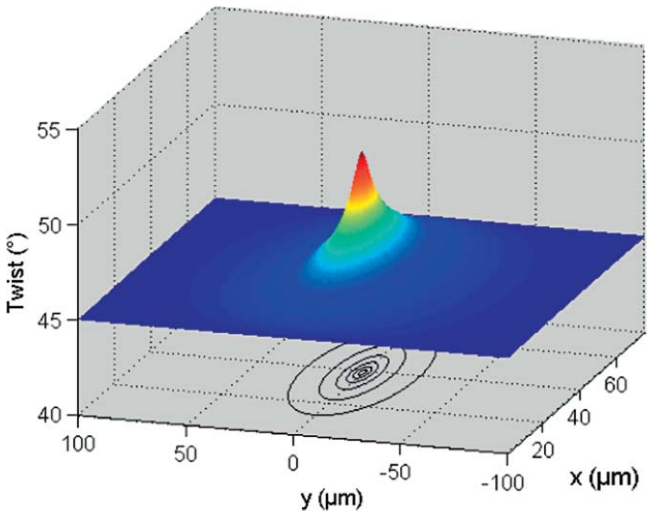

Fig. 18 Distribution of the director angle in a cell with uniform orientation of 45 deg. A Gaussian beam of 3 μm waist with an electric field along the *y* direction reorients the director.

propagation direction of the light and the electric field. The optical electric field reorients the director not only exactly at the position of the light beam, but in a much larger area, caused by the elastic forces between the LC molecules, as shown in Fig. 18. The area or reorientation is much larger than the beam width,[154–156] and in nonlinear optics, one speaks about a highly nonlocal nonlinearity. The high nonlocality is advantageous because this effect leads to highly stable solitons.[157] The propagation of the Gaussian beam is visualized in Fig. 19 by means of a numerical model.[150] It is clearly visible that, for low optical power, the beam width increases along the propagation direction, while an optical power of 3.5 mW leads to a well-confined beam profile along the propagation direction. Note that there is a slight walk-off angle due to the anisotropy of the LC.[158,159] Also in polymer-stabilized liquid crystal, the generation of spatial solitons has been reported.[160]

Thermal solitons rely on the fact that the ordinary index of refraction increases with temperature, as shown in Fig. 15. The optical beam is heating the cell that gives rise

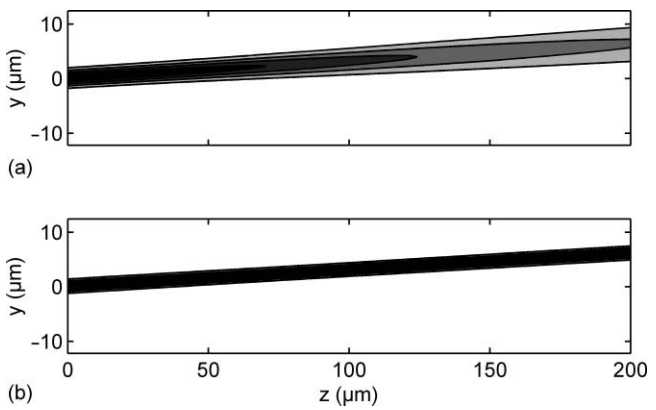

Fig. 19 Propagation of a Gaussian beam of 3 μm waist in a cell with (a) 45 deg orientation of the director for no nonlinearity and (b) for 3.5 -mW optical power.

to a certain temperature profile. Usually, an absorbing dye is mixed with the LC in order to facilitate the thermal effect. In this way, soliton generation is possible for a few milliwatts of optical power, similar to the reorientational solitons. The temperature profile is governed by a diffusion equation, and the nonlinearity is thus again highly nonlocal.[161–163] Azobenzene liquid-crystals are very sensitive to light of certain wavelength. An optical beam in the green spectrum gives rise to an increase of cis-molecules in the solution, while a red laser beam gives rise to an increase in transmolecules. When the polarization of light is parallel to the director and a red laser beam is used, one thus obtains a positive nonlinearity or self-focusing and a spatial soliton can be generated.[164] The necessary optical power is on the order of tens of microwatts. Because there is a continuous diffusion and generation of transmolecules, the solitons are not completely stable in time. A possible advantage of working with azobenzene LCs is that the cis-transisomerization process can be very fast, on the order of nanoseconds.[133]

The main applications of spatial solitons are in the domain of reconfigurable optical interconnects. It is possible to steer or switch the solitons by means of interaction with other light beams[165,166] or by using an applied electric field.[167] An important phenomenon is the attraction between two soliton beams due to the high nonlocality. Not only do two solitons propagating in the same direction attract each other,[168] counterpropagating solitons also attract and even merge if the distance and angle mismatch are not too large. Guiding light from one fiber into the other with the help of soliton attraction was shown in Ref. 162, proving the possibility of making optical interconnects with less stringent mechanical accuracy. In Ref. 169 it was demonstrated that a the self-induced waveguide created by the soliton can be succesfully used to enhance the recovery of fluorescent light. But probably the most important merit of nematicons is that several nonlinear optical phenomena can be investigated without the need for high peak-power pulsed laser sources, such as modulation instability[170–172] and discrete solitons.[173]

8 Conclusions and Outlook

The breakthrough of liquid-crystal devices during the past two decades is remarkable. Next to liquid-crystal displays, which have led to a new era in the mobile and display market segment, the excellent electro-optic properties of liquid-crystals have been widely applied to design tunable photonic components. This review has given a broad overview of these recent applications, which range from optical filters and switches to spatial light modulators, waveguide-based devices and applications employing the strong optical nonlinearity of liquid-crystals. In the future, new opportunities certainly arise from the rich behavior of polymerizable liquid-crystals and the stabilization of liquid-crystal blue phases with their unique properties over a wide temperature range. Other fascinating routes are to control the creation of defects in nematic liquid-crystals (induced electrically or by structure features), which may allow the development of new bistable devices, or the inclusion of nanoparticles, which are dielectric, ferroelectric, or magnetic to improve LC properties. Obviously, the fascinating research field of liquid-crystal–based photonic applications is rapidly evolving and the emerging devices are likely to become key components to perform manipulation of light.

Acknowledgments

Jeroen Beeckman is Postdoctoral Fellow of the Research Foundation - Flanders (FWO) and Pieter Vanbrabant is PhD fellow of the same institution. This research is the result of collaboration within the IAP project Photonics@be of the Belgian Science Policy Office.

References

1. C. L. van Oosten, D. Corbett, D. Davies, M. Warner, C. W. M. Bastiaansen, and D. J. Broer, "Bending dynamics and directionality reversal in liquid-crystal network photoactuators", *Macromolecules* **41**, 8592–8596 (2008).
2. H. Finkelmann, E. Nishikawa, G. G. Pereira, and M. Warner, "A new opto-mechanical effect in solids", *Phys. Rev. Lett.* **87**, 015501 (2001).
3. Y. L. Yu, M. Nakano, and T. Ikeda, "Directed bending of a polymer film by light—miniaturizing a simple photomechanical system could expand its range of applications." *Nature* **425**, 145–145 (2003).
4. D. J. Broer, J. Lub, and G. N. Mol, "Wide-band reflective polarizers from cholesteric polymer networks with a pitch gradient", *Nature* **378**, 467–469 (1995).
5. T. J. White, A. S. Freer, N. V. Tabiryan, and T. J. Bunning, "Photoinduced broadening of cholesteric liquid-crystal reflectors", *J. Appl. Phys.* **107**, 073110 (2010).
6. P. G. de Gennes and J. Prost, *The Physics of Liquid-Crystals*, Oxford University Press, Oxford, 1995).
7. I. C. Khoo, *Liquid-Crystals: Physical Properties and Nonlinear Optical Phenomena*, Wiley Hoboken, NJ (1994).
8. I. Dierking, *Textures of Liquid-Crystals*, Wiley-VCH Verlag, Weinheim (2003).
9. E. Lueder, *Liquid–Crystal Displays: Addressing Schemes and Electro-Optical Effects*, Wiley, Chichester (2001).
10. P. Yeh and C. Gu, *Optics of Liquid–Crystal Displays*, (Wiley Hoboken, NJ (2010).
11. Z. Ge and S.-T. Wu, *Transflective Liquid–Crystal Displays*, (Wiley, Hoboken, NJ (2010).
12. J. L. de Bougrenet de la Tocnaye, "Engineering liquid-crystals for optimal uses in optical communication systems", *Liq. Cryst.* **31**, 241–269 (2004).
13. P. J. Collings and M. Hird, *Introduction to Liquid-Crystals: Chemistry and Physics*, Taylor and Francis, New York (2004).
14. D. R. Lovett, *Tensor properties of crystals* Institute of Physics Publishing, Bristol (1989).
15. D. A. Dunmur, A. Fukuda, and G. R. Luckhurst, eds., *Physical properties of liquid-crystals: nematics* (INSPEC, London, 2001).
16. P. J. Shannon, W. M. Gibbons, and S. T. Sun, "Patterned optical-properties in photopolymerized surface-aligned liquid-crystal films", *Nature* **368**, 532–533 (1994).
17. C. Oh and M. J. Escuti, "Achromatic diffraction from polarization gratings with high efficiency", *Opt. Lett.* **33**, 2287–2289 (2008).
18. S. R. Nersisyan, N. V. Tabiryan, D. M. Steeves, and B. R. Kimball, "Characterization of optically imprinted polarization gratings", *Appl. Opt.* **48**, 4062–4067 (2009).
19. X. J. Zhao, A. Bermak, F. Boussaid, T. Du, and V. G. Chigrinov, "High-resolution photoaligned liquid-crystal micropolarizer array for polarization imaging in visible spectrum", *Opt. Lett.* **34**, 3619–3621 (2009).
20. L. M. Blinov and V. G. Chigrinov, *Electrooptic Effects in Liquid–Crystal Materials* (Springer-Verlag, Berlin 1994).
21. S. Chandrasekhar, *liquid-crystals*, (2nd ed.) Cambridge University Press, Cambridge, England (1992).
22. H. Kikuchi, M. Yokota, Y. Hisakado, H. Yang, and T. Kajiyama, "Polymer-stabilized liquid-crystal blue phases", *Nat. Mater.* **1**, 64–68 (2002).
23. H. J. Coles and M. N. Pivnenko, "liquid-crystal 'blue phases' with a wide temperature range", *Nature* **436**, 997–1000 (2005).
24. Y. Ohman, "A new monochromator", *Nature* **157**, 291 (1938).
25. J. Beeckman, T. Hui, P. J. M. Vanbrabant, R. Zmijan, and K. Neyts, "Polarization selective wavelength tunable filter", *Mol. Cryst. Liq. Cryst.* **502**, 19–28 (2009).
26. A. Safrani and I. Abdulhalim, "Spectropolarimetric method for optic axis, retardation, and birefringence dispersion measurement", *Opt. Eng.* **48**, 053601 (2009).
27. I. Abdulhalim, "Unique optical properties of anisotropic helical structures in a Fabry–Perot cavity", *Opt. Lett.* **31**, 3019–3021 (2006).
28. O. Aharon and I. Abdulhalim, "Tunable optical filter having a large dynamic range", *Opt. Lett.* **34**, 2114–2116 (2009).
29. O. Aharon and I. Abdulhalim, "liquid-crystal lyot tunable filter with extended free spectral range", *Opt. Express* **17**, 11426–11433 (2009).
30. O. Aharon and I. Abdulhalim, "liquid-crystal wavelength-independent continuous polarization rotator", *Optical Engineering* **49**, 034002 (2010).
31. J. Beeckman, D. P. Medialdea, T. Hui, K. Neyts, and X. Quintana, "Fast visible-near infrared switchable liquid-crystal filter", *Mol. Cryst. Liq. Cryst.* **502**, 9–18 (2009).
32. G. Abbate, F. Vita, A. Marino, V. Tkachenko, S. Slussarenko, O. Sakhno, and J. Stumpe, "New generation of holographic gratings based on polymer-lc composites: policryps and poliphem", *Mol. Cryst. Liq. Cryst.* **453**, 1–13 (2006).
33. A. E. Fox, K. Rai, and A. K. Fontecchio, "Holographically formed polymer dispersed liquid-crystal films for transmission mode spectrometer applications", *Appl. Opt.* **46**, 6277–6282 (2007).
34. C. Peralta, A. Pons, and J. Campos, "How the method of choice to assess liquid-crystal tunable filters' bandpass function impacts the spectroradiometric measurements performed with them", *J. Opt.* **12**, 015707 (2010).
35. A. d'Alessandro and R. Asquini, "liquid-crystal devices for photonic switching applications: State of the art and future developments", *Mol. Cryst. Liq. Cryst.* **398**, 207–221 (2003).
36. C. Vazquez, J. M. S Pena, and A. L. Aranda, "Broadband 1 x 2 polymer optical fiber switches using nematic liquid-crystals", *Opt. Commun.* **224**, 57–62 (2003).
37. P. C. Lallana, C. Vazquez, J. M. S. Pena, and R. Vergaz, "Reconfigurable optical multiplexer based on liquid-crystals for polymer optical fiber networks", *Opto-Electron. Rev.* **14**, 311–318 (2006).
38. J. B. Yang, X. J. Li, J. K. Yang, J. Liu, and X. Y. Su, "Polarization-independent bidirectional 4 x 4 optical switch in free space", *Opt. Laser Technol.* **42**, 927–933 (2010).
39. W. A. Crossland, I. G. Manolis, M. M. Redmond, K. L. Tan, T. D. Wilkinson, M. J. Holmes, T. R. Parker, H. H. Chu, J. Croucher, V. A. Handerek, S. T. Warr, B. Robertson, I. G. Bonas, R. Franklin, C. Stace, H. J. White, R. A. Woolley, and G. Henshall, "Holographic optical switching: The 'roses' demonstrator", *J. Lightwave Technol.* **18**, 1845–1854 (2000).
40. C. J. Henderson, D. G. Leyva, and T. D. Wilkinson, "Free space adaptive optical interconnect at 1.25 gb/s, with beam steering using a ferroelectric liquid-crystal slm", *J. Lightwave Technol.* **24**, 1989–1997 (2006).
41. J. J. Chen and K. H. Cheng, "Light-emitting diode cover lens design for large-scale liquid-crystal device television backlight", *Opt. Eng.* **49**, 053003 (2010).
42. N. A. Riza, M. Sheikh, G. Webb-Wood, and P. G. Kik, "Demonstration of three-dimensional optical imaging using a confocal microscope based on a liquid-crystal electronic lens", *Opt. Eng.* **47**, 063201 (2008).
43. S. Sato, "Liquid-crystal lens-cells with variable focal length", *J. J. Appl. Phys.* **18**, 1679–1684 (1979).
44. H. W. Ren and S. T. Wu, "Adaptive liquid-crystal lens with large focal length tunability", *Opt. Express* **14**, 11292–11298 (2006).
45. K. Asatryan, V. Presnyakov, A. Tork, A. Zohrabyan, A. Bagramyan, and T. Galstian, "Optical lens with electrically variable focus using an optically hidden dielectric structure", *Opt. Express* **18**, 13981–13992 (2010).
46. N. Fraval and J. L. D. de la Tocnaye, "Low aberrations symmetrical adaptive modal liquid-crystal lens with short focal lengths", *Appl. Opt.* **49**, 2778–2783 (2010).
47. M. Ye and S. Sato, "liquid-crystal lens with focus movable along and off axis", *Opt. Commun.* **225**, 277–280 (2003).
48. M. Ye, B. Wang, and S. Sato, "Realization of liquid-crystal lens of large aperture and low driving voltages using thin layer of weakly conductive material", *Opt. Express* **16**, 4302–4308 (2008).
49. P. Valley, D. L. Mathine, M. R. Dodge, J. Schwiegerling, G. Peyman, and N. Peyghambarian, "Tunable-focus flat liquid-crystal diffractive lens", *Opt. Lett.* **35**, 336–338 (2010).
50. V. V. Presnyakov, K. E. Asatryan, T. V. Galstian, and A. Tork, "Polymer-stabilized liquid-crystal for tunable microlens applications", *Opt. Express* **10**, 865–870 (2002).
51. H. W. Ren and S. T. Wu, "Tunable electronic lens using a gradient polymer network liquid-crystal", *Appl. Phys. Lett.* **82**, 22–24 (2003).
52. P. F. McManamon, P. J. Bos, M. J. Escuti, J. Heikenfeld, S. Serati, H. Xie, and E. A. Watson, "A review of phased array steering for narrow-band electrooptical systems", *Proc. IEEE* **97**, 1078–1096 (2009).
53. P. F. McManamon, E. A. Watson, T. A. Dorschner, and L. J. Barnes, "Applications look at the use of liquid-crystal writable gratings for steering passive radiation", *Opt. Eng.* **32**, 2657–2667 (1993).
54. I. G. Manolis, T. D. Wilkinson, M. M. Redmond, and W. A. Crossland, "Reconfigurable multilevel phase holograms for optical switches", *IEEE Photon. Technol. Lett.* **14**, 801–803 (2002).
55. S. Ahderom, M. Raisi, K. Alameh, and K. Eshraghian, "Dynamic wdm equalizer using opto-VLSI beam processing", *IEEE Photon. Technol. Lett.* **15**, 1603–1605 (2003).
56. M. Aljada, K. Alameh, Y. T. Lee, and I. S. Chung, "High-speed (2.5ghz) reconfigurable inter-chip optical interconnects using opto-vlsi processors", *Opt. Express* **14**, 6823–6836 (2006).
57. E. A. Watson and L. J. Barnes, "Optical design considerations for agile beam steering", *Proc. SPIE* **2120**, 186–193 (1994).
58. P. F. McManamon, T. A. Dorschner, D. C. Corkum, L. J. Friedman, D. S. Hobbs, M. K.O. Holz, S. Liberman, H. Nguyen, D. P. Resler,

R. C. Sharp, and E. A. Watson, "Optical phased array technology", *Proc. IEEE* **84**, 268–298 (1996).
59. R. C. Sharp, D. P. Resler, D. S. Hobbs, and T. A. Dorschner, "Electrically tunable liquid-crystal wave plate in the infrared", *Opt. Lett.* **15**, 87–89 (1990).
60. D. P. Resler, D. S. Hobbs, R. C. Sharp, L. J. Friedman, , and T. A. Dorschner, "High-efficiency liquid-crystal optical phased-array beam steering", *Opt. Lett.* **21**, 689–691 (1996).
61. R. M. Matic, "Blazed phased liquid-crystal beam steering", *Proc. SPIE* **2120**, 194–205 (1994).
62. P. F. McManamon, "Agile nonmechanical beam steering", *Opt. Photon. News* **3**, 21–25 (March 2006).
63. R. James, F. A. Fernandez, S. E. Day, M. Komarcevic, and W. A. Crossland, "Modeling of the diffraction efficiency and polarization sensitivity for a liquid-crystal 2d spatial light modulator for reconfigurable beam steering", *Opt. Soc. Am.* **24**, 2464–2473 (2007).
64. P. J.M. Vanbrabant, J. Beeckman, K. Neyts, R. James, and F. A. Fernandez, "A finite element beam propagation method for simulation of liquid-crystal devices", *Opt. Express* **17**, 10895–10909 (2009).
65. P. J.M. Vanbrabant, J. Beeckman, K. Neyts, E. Willman, and F. A. Fernandez, "Diffraction and fringing field effects in small pixel liquid-crystal devices with homeotropic alignment", *J. Appl. Phys.* **108**, 083104 (2010).
66. S. Harris, "Polarization effects in nematic liquid-crystal optical phased arrays", *Proc. IEEE* **5213**, 26–39 (2004).
67. A. Lizana, N. Martin, M. Estape, E. Fernandez, I. Moreno, A. Marquez, C. Iemmi, J. Campos, and M. J. Yzuel, "Influence of the incident angle in the performance of liquid-crystal on silicon displays", *Opt. Express* **17**, 8491–8505 (2009).
68. X. Wang, B. Wang, P. J. Bos, P. F. McManamon, J. J. Pouch, F. A. Miranda, and J. E. Anderson, "Modeling and design of an optimized liquid-crystal optical phased array", *J. Appl. Phys.* **98**, 073101 (2005).
69. J. R. Moore, N. Collings, W. A. Crossland, A. B. Davey, M. Evans, A. M. Jeziorska, M. Komarcevic, R. J. Parker, T. D. Wilkinson, and H. Xu, "The silicon baekplane design for an lcos polarization-insensitive phase hologram slm", *IEEE Photon. Technol. Lett.* **20**, 60–62 (2008).
70. T. A. Dorschner and D. P. Resler, "Optical beam steerer having subaperture addressing", US Patent No. 5 093 740 (1992).
71. C. M. Titus, P. J. Bos, and O. D. Lavrentovich, "Efficient, accurate liquid-crystal digital light reflector", *Proc. SPIE* **3633**, 244–253 (1999).
72. S. A. Khan and N. A. Riza, "Demonstration of 3-dimensional wide angle laser beam scanner using liquid-crystals", *Opt. Express* **12**, 868–882 (2004).
73. J. Kim, C. Oh, M. J. Escuti, L. Hosting, and S. Serati, "Wide angle nonmechanical beam steering using thin liquid-crystal polarization gratings", *Proc. SPIE* **7093**, 709302 (2008).
74. M. J. Escuti and W. M. Jones, "Polarization independent switching with high contrast from a liquid-crystal polarization grating", *SID Symp. Dig. Tech. Papers* **37**, 1443–1446 (2006).
75. R. Komanduri, W. M. Jones, C. Oh, and M. J. Escuti, "Polarization-independent modulation for projection displays using small-period lc polarization gratings", *J. Soc. Inf. Display* **15**, 589–594 (2007).
76. I. W. Smith and M. K.O. Holz, "Wide angle beam steering system", US Patent No. 7 215 472 (2007).
77. H. Kogelnik, "Coupled wave theory for thick hologram gratings", *Bell Syst. Tech. J.* **48**, 2909–2947 (1969).
78. I. V. Ciapurin, L. B. Glebov, and V. I. Smirnov, "Modeling of Gaussian beam diffraction on volume bragg gratings in PTR glass", *Proc. SPIE* **5742**, 591215 (2005).
79. R. Gerchberg and W. Saxton, "Practical algorithm for determination of phase from image and diffraction plane pictures", *OPTIK* **35**, 237–246 (1972).
80. A. Jesacher, C. Maurer, A. Schwaighofer, S. Bernet, and M. Ritsch-Marte, "Near-perfect hologram reconstruction with a spatial light modulator", *Opt. Express* **16**, 2597–2603 (2008).
81. V. A. Soifer, *Methods for Computer Design of Diffractive Optical Elements*, Wiley, Hoboken, NJ, New York, 2002).
82. J. C. Pizolato and L. G. Neto, "Phase-only optical encryption based on the zeroth-order phase-contrast technique", *Opt. Eng.* **48**, 098201 (2009).
83. M. Madec, W. Uhring, E. Hueber, J. B. Fasquel, J. Bartringer, and Y. Herve, "Methods for improvement of spatial light modulator image rendering", *Opt. Eng.* **48**, 034002 (2009).
84. E. Frumker and Y. Silberberg, "Phase and amplitude pulse shaping with two-dimensional phase-only spatial light modulators", *J. Opt. Soc. Am. B* **24**, 2940–2947 (2007).
85. A. Martinez-Garcia, J. L. Martinez, P. Garcia-Martinez, M. D. Sanchez-Lopez, and I. Moreno, "Time-multiplexed chromatic-controlled axial diffractive optical elements", *Opt. Eng.* **49**, 078201 (2010).
86. G. Curatu and J. E. Harvey, "Analysis and design of wide-angle foveated optical systems based on transmissive liquid-crystal spatial light modulators", *Opt. Eng.* **48**, 043001 (2009).
87. G. D. Love, "Wave-front correction and production of zernike modes with a liquid-crystal spatial light modulator", *Appl. Opt.* **36**, 1517–1520 (1997).
88. L. P. Zhao, N. Bai, X. Li, L. S. Ong, Z. P. Fang, and A. K. Asundi, "Efficient implementation of a spatial light modulator as a diffractive optical microlens array in a digital Shack–Hartmann wavefront sensor", *Appl. Opt.* **45**, 90–64 (2006).
89. K. Obata, J. Koch, U. Hinze, and B. N. Chichkov, "Multi-focus two-photon polymerization technique based on individually controlled phase modulation", *Opt. Express* **18**, 17193–17200 (2010).
90. C. Bay, N. Huebner, J. Freeman, and T. Wilkinson, "Maskless photolithography via holographic optical projection", *Opt. Lett.* **35**, 2230–2232 (2010).
91. E. Buckley, "Holographic laser projection technology", *SID Int. Symp. Digest Tech. Papers* **39**, 1074–1079 (2008).
92. A. Georgiou, T. DWilkinson, N. Collings, and W. A. Crossland, "An algorithm for computing spot-generating holograms", *J. Opt. A: Pure Appl. Opt.* **10**, 015306 (2008).
93. A. Ashkin, J. M. Dziedzic, J. E. Bjorkholm, and S. Chu, "Observation of a single-beam gradient force optical trap for dielectric particles", *Opt. Lett.* **11**, 288–290 (1986).
94. T.-H. Chao, T. T. Lu, S. R. Davis, S. D. Rommel, G. Farca, B. Luey, A. Martin, and M. H. Anderson, "Compact liquid-crystal waveguide based fourier transform spectrometer for in-situ and remote gas and chemical sensing", *Proc. SPIE* 69770p (2008).
95. N. A. Clark and M. A. Handshy, "Surface-stabilized ferroelectric liquid-crystal electro-optic waveguide switch", *Appl. Phys. Lett.* **57**, 1852–1854 (1990).
96. G. N. Ntogari, D. Tsipouridou, and E. Kriezis, "A numerical study of optical switches and modulators based on ferroelectric liquid-crystals", *J. Opt. A: Pure Appl. Opt.* **7**, 82–87 (2005).
97. H. Desmet, K. Neyts, and R. Baets, "Modeling nematic liquid-crystals in the neighborhood of edges", *J. Appl. Phys.* **98**, 123517 (2005).
98. H. Desmet, W. Bogaerts, A. Adamski, J. Beeckman, K. Neyts, and R. Baets, "Silicon-on-insulator optical waveguides with liquid-crystal cladding for switching and tuning", in *Proc. Euro. Conf. on Opt. Commun.*, Vol. **3** pp. 430–431 (2003).
99. W. De Cort, J. Beeckman, R James, F. A. Fernandez, R. Baets, and K. Neyts, "Tuning of silicon-on-insulator ring resonators with liquid-crystal cladding using the longitudinal field component", *Opt. Lett.* **34**, 2054–2056 (2009).
100. V. G. Chigrinov, L. Zhou, A. A. Muravsky, and A. W. Poon, "*Electrically tunable microresonators using photoaligned liquid-crystals*," *On US Patent* 7, 783,144 B2 (2010).
101. A. Di Falco and G. Assanto, "Tunable wavelength-selective add-drop in liquid-crystals on a silicon microresonator", *Opt. Commun.* **279**, 210–213 (2007).
102. L. Sirleto, G. Coppola, and G. Breglio, "Optical multimode interference router based on a liquid-crystal waveguide", *J. Opt. A* **5**, S298–S304 (2003).
103. A. Fratalocchi, R. Asquini, and G. Assanto, "Integrated electro-optic switch in liquid-crystals", *Opt. Express* **13**, 32–36 (2005)
104. A. d'Alessandro, B. Bellini, D. Donisi, R. Beccherelli, and R. Asquini, "Nematic liquid-crystal optical channel waveguides on silicon", *IEEE J. Quantum Electron.* **42**, 1084–1090 (2006).
105. Y. P. Lan, C. Y. Chen, R. P. Pan, and C. L. Pan, "Fine-tuning of a diode laser wavelength with a liquid-crystal intracavity element", *Opt. Eng.* **43**, 234–238 (2004).
106. T. S. Shih, Y. P. Lan, Y. F. Lin, R. P. Pan, and C. L. Pan, "Single-longitudinal-mode semiconductor laser with digital and mode-hop-free fine-tuning mechanisms", *Opt. Express* **12**, 6434–6439 (2004).
107. C. Levallois, B. Caillaud, J. L. de Bougrenet de la Tocnaye, L. Dupont, A. Le Corre, H. Folliot, O. Dehaese, and S. Loualiche, "Long-wavelength vertical-cavity surface-emitting laser using an electro-optic index modulator with 10 nm tuning range", *Appl. Phys. Lett.* **89**, 011102 (2006).
108. K. Sato, K. Mizutani, S. Sudo, K. Tsuruoka, K. Naniwae, and K. Kudo, "Wideband external cavity wavelength-tunable laser utilizing a liquid-crystal-based mirror and an intracavity etalon", *J. Lightwave Technol* **25**, 2226–2232 (2007).
109. P. Wang, L. K. Seah, V. M. Murukeshan, and Z. X. Chao, "Electronically tunable external-cavity laser diode using a liquid-crystal deflector", *IEEE Photon. Technol. Lett.* **18**, 1612–1614 (2006).
110. C. B. Olausson, L. Scolari, L. Wei, D. Noordegraaf, J. Weirich, T. T. Alkeskjold, K. P. Hansen, and A. Bjarklev, "Electrically tunable yb-doped fiber laser based on a liquid-crystal photonic bandgap fiber device", *Opt. Express* **18**, 8229–8238 (2010).
111. I. P. Ilchishin, E. A. Tikhonov, V. G. Tischenko, and M. T. Shpak, "Generation of a tunable radiation by impurity cholesteric liquid-crystals", *JETP Lett.* **32**, 24–27 (1980).
112. A. D. Ford, S. M. Morris, and H. J. Coles, "Photonics and lasing in liquid-crystals", *Mater. Today* **9**, 36–42 (2006).
113. H. Coles and S. Morris, "Liquid-crystal lasers", *Nat. Photon.* **4**, 676–685 (2010).
114. V. Barna, R. Caputo, A. De Luca, N. Scaramuzza, G. Strangi, C. Versace, C. Umeton, R. Bartolino, and G. N. Price, "Distributed feedback

micro-laser array: helixed liquid-crystals embedded in holographically sculptured polymeric microcavities", *Opt. Express* **14**, 2695–2705 (2006).
115. A. Chanishvili, G. Chilaya, G. Petriashvili, R. Barberi, R. Bartolino, G. Cipparrone, A. Mazzulla, R. Gimenez, L. Oriol, and M. Pinol, "Widely tunable ultraviolet-visible liquid-crystal laser", *Appl. Phys. Lett.* **86**, 051107 (2005).
116. A. Chanishvili, G. Chilaya, G. Petriashvili, R. Barberi, R. Bartolino, G. Cipparrone, A. Mazzulla, and L. Oriol, "Lasing in dye-doped cholesteric liquid-crystals: two new tuning strategies", *Adv. Mater.* **16**, 791–795 (2004).
117. S. H. Lin, C. Y. Shyu, J. H. Liu, P. C. Yang, T. S. Mo, S. Y. Huang, and C. R. Lee, "Photoerasable and photorewritable spatially-tunable laser based on a dye-doped cholesteric liquid-crystal with a photoisomerizable chiral dopant", *Opt. Express* **18**, 9496–9503 (2010).
118. S. Furumi, S. Yokoyama, A. Otomo, and S. Mashiko, "Electrical control of the structure and lasing in chiral photonic band-gap liquid-crystals", *Appl. Phys. Lett.* **82**, 16–18 (2003).
119. T. H. Lin, H. C. Jau, C. H. Chen, Y. J. Chen, T. H. Wei, C. W. Chen, and A. Y.G. Fuh, "Electrically controllable laser based on cholesteric liquid-crystal with negative dielectric anisotropy", *Applied Physics Letters* **88**, 061122 (2006).
120. M. Kasano, M. Ozaki, K. Yoshino, D. Ganzke, and W. Haase, "Electrically tunable waveguide laser based on ferroelectric liquid-crystal", *Applied Physics Letters* **82**, 4026–4028 (2003).
121. G. Strangi, S. Ferjani, V. Barna, A. De Luca, C. Versace, N. Scaramuzza, and R. Bartolino, "Random lasing and weak localization of light in dye-doped nematic liquid-crystals", *Opt. Express* **14**, 7737–7744 (2006).
122. S. Ferjani, V. Barna, A. De Luca, C. Versace, and G. Strangi, "Random lasing in freely suspended dye-doped nematic liquid-crystals", *Opt. Lett.* **33**, 557–559 (2008).
123. M. V. Vasnetsov, S. S. Slussarenko, J. Stumpe, O. Sakhno, S. S. Slussarenko, and G. Abbate, "Lasing by second-order bragg diffraction in dye-doped poliphem gratings", *Mol. Cryst. Liq. Cryst.* **516**, 159–166 (2010).
124. I. C. Khoo, "Nonlinear optics of liquid-crystalline materials", *Phys. Rep.* **471**, 221–267 (2009).
125. F. Simoni, *Nonlinear Optical Properties of liquid-crystals and Polymer Dispersed Liquid-CrystalsLiquid–Crystals* World Sci., Singapore (1997).
126. W. Chen, M. B. Feller, and Y. R. Shen, "Investigation of anisotropic molecular orientational distributions of liquid-crystal monolayers by optical second-harmonic generation", *Phys. Rev. Lett.* **65**, 2665–2668 (1989).
127. I. C. Pintre, J. L. Serrano, M. B. Ros, J. Martinez-Perdiguero, I. Alonso, J. Ortega, C. L. Folcia, J. Etxebarria, R. Alicante, and B. Villacampa, "Bent-core liquid-crystals in a route to efficient organic nonlinear optical materials", *J. Mater. Chem.* **20**, 2965–2971 (2010).
128. G. P. Agrawal, *Nonlinear Fiber Optics*, ed. Academic Press, New York, (2001).
129. J. Philip and T. A.P. Rao, "Nonresonant 3rd-order susceptibility measurements in the nematic liquid-crystal k18", *Opt. Quantum Electron.* **25**, 157–162 (1993).
130. I. Jánossy, "Molecular interpretation of the absorption induced reorientation of nematic liquid-crystals", *Phys. Rev. E* **49**, 2957–2963 (1994).
131. O. Baldovino-Pantaleon, R. Porras-Aguilar, A. Sanchez-Castillo, J. C. Ramirez-San-Juan, R. Ramos-Garcia, and E. A. Gonzalez, "Anchoring of 4-dimethyl-amino substituted azobenzene dyes doped liquid-crystals on substrates", *Mol. Cryst. Liq. Cryst.* **488**, 1–10 (2008).
132. C. Manzo, D. Paparo, L. Marrucci, and I. Janossy, "Light-induced rotation of dye-doped liquid-crystal droplets", *Phys. Rev. E* **73**, 051707 (2006).
133. U. Hrozhyka, S. Seraka, N. Tabiryana, L. Hokeb, D. M. Steevesb, G. Kedziorac, and B. Kimball, "High optical nonlinearity of azobenzene liquid-crystals for short laser pulses", *Proc. SPIE* **7050**, 705007 (2008).
134. I. C. Khoo, H. Li, and Y. Liang, "Observation of orientational photorefractive effects in nematic liquid cyrstals", *Opt. Lett.* **19**, 1723–1725 (1994).
135. M. Kaczmarek, A. Dyadyusha, S. Slussarenko, and I. C. Khoo, "The role of surface charge field in two-beam coupling in liquid-crystal cells with photoconducting polymer layers", *J. Appl. Phys.* **96**, 2616–2623 (2004).
136. X. D. Sun, C. Y. Ren, Y. B. Pei, and F. F. Yao, "Electrically controlled dynamic holographic gratings in fullerene c-60-doped nematic liquid-crystals", *J. Phys.* **41**, 245105 (2008).
137. I. C. Khoo, "Holographic grating formation in dye- and fullerene c60-doped nematic liquid-crystal film", *Opt. Lett.* **20**, 2137–2139 (1995).
138. F. Simoni, L. Lucchetti, D. E. Lucchetta, and O. Francescangeli, "On the origin of the huge nonlinear response of dye-doped liquid-crystals", *Optics Express* **9**, 85–90 (2001).
139. I. C. Khoo, M. V. Wood, M. Y. Shih, and P. H. Shen, "Extremely nonlinear photosensitive liquid-crystals for image sensing and sensor protection", *Opt. Express* **4**, 432–442 (1999).
140. G. Cook, A. V. Glushchenko, V. Reshetnyak, A. T. Griffith, M. A. Saleh, and D. R. Evans, "Nanoparticle doped organic-inorganic hybrid photorefractives", *Optics Express* **16**, 4015–4022 (2008).
141. Y. S. Kivshar and G. P. Agrawal, *Optical Solitons – From Fibers to Photonic Crystals* (Academic Press, New York, 2003).
142. G. I. Stegeman, D. N. Christodoulides, and M. Segev, "Optical spatial solitons: Historical perspectives", *IEEE J. Sel. Top. Quantum. Electron.* **6**, 1419–1427 (2000).
143. A. W. Snyder, D. J. Mitchell, L. Poladian, and F. Ladouceur, "Self-induced optical fibers — spatial solitary waves", *Opt. Lett.* **16**, 21–23 (1991).
144. G. Assanto, M. Peccianti, and C. Conti, "Nematicons: Optical spatial solitons in nematic liquid-crystals", *Opt. Photon. News* **14**(2), 44–48 (2003).
145. M. A. Karpierz, M. Sierakowski, M. Swillo, and T. Wolinsky, "Self-focusing in liquid-crystalline waveguides", *Mol. Cryst. Liq. Cryst.* **320**, 157–163 (1998).
146. M. Peccianti, A. De Rossi, G. Assanto, A. De Luca, C. Umeton, and I. C. Khoo, "Electrically assisted self-confinement and waveguiding in planar nematic liquid-crystal cells", *Appl. Phys. Lett.* **77**, 7–9 (2000).
147. M. Peccianti, C. Conti, G. Assanto, A. De Luca, and C. Umeton, "Routing of anisotropic spatial solitons and modulational instability in liquid-crystals", *Nature* **432**, 733–737 (2004).
148. M. A. Karpierz, "Solitary waves in liquid-crystalline waveguides", *Phys. Rev. E* **66**, 036603 (2002).
149. U. A. Laudyn, M. Kwasny, and M. A. Karpierz, "Nematicons in chiral nematic liquid-crystals", *Appl. Phys. Lett.* **94**, 091110 (2009).
150. J. Beeckman, K. Neyts, X. Hutsebaut, C. Cambournac, and M. Haelterman, "Simulations and experiments on self-focusing conditions in nematic liquid-crystal planar cells", *Opt. Express* **12**, 1011–1018 (2004).
151. J. Beeckman, K. Neyts, X. Hutsebaut, and M. Haelterman, "Observation of out-coupling of a nematicon", *Opto-Electron. Rev.* **14**, 263–267 (2006).
152. A. I. Strinić, D. V. Timotijević, D. Arsenović, M. S. Petrović, and M. R. Belić, "Spatiotemporal optical instabilities in nematic solitons", *Opt. Express* **13**, 493–504 (2005).
153. Y. V. Izdebskaya, V. G. Shvedov, A. S. Desyatnikov, W. Z. Krolikowski, M. Belic, G. Assanto, and Y. S. Kivshar, "Counterpropagating nematicons in bias-free liquid-crystals", *Opt. Express* **18**, 3258–3263 (2010).
154. C. Conti, M. Peccianti, and G. Assanto, "Observation of optical spatial solitons in a highly nonlocal medium", *Phys. Rev. Lett.* **92**, 113902 (2004).
155. X. Hutsebaut, C. Cambournac, M. Haelterman, J. Beeckman, and K. Neyts, "Measurement of the self-induced waveguide of a solitonlike optical beam in a nematic liquid-crystal", *J. Opt. Soc. Am. B* **22**, 1424–1431 (2005).
156. J. F. Henninot, J. F. Blach, and M. Warenghem, "Experimental study of the nonlocality of spatial optical solitons excited in nematic liquid-crystal", *J. Opt. A* **9**, 20–25 (2007).
157. A. W. Snyder and D. J. Mitchell, "Accessible solitons", *Science* **276**, 1538–1541 (1997).
158. J. Beeckman, K. Neyts, X. Hutsebaut, C. Cambournac, and M. Haelterman, "Simulation of 2-D lateral light propagation in nematic-liquid-crystal cells with tilted molecules and nonlinear reorientational effect", *Opt. Quantum Electron.* **37**, 95–106 (2005).
159. M. Peccianti, A. Fratalocchi, and G. Assanto, "Transverse dynamics of nematicons", *Opt. Express* **12**, 6524–6529 (2004).
160. J. F. Blach, J. F. Henninot, M. Petit, A. Daoudi, and M. Warenghem, "Observation of spatial optical solitons launched in biased and bias-free polymer-stabilized nematics", *J. Opt. Soc. Am. B* **24**, 1122–1129 (2007).
161. M. Warenghem, J. F. Henninot, and G. Abbate, "Nonlinearly induced self waveguiding structure in dye doped nematic liquid-crystals confined in capillaries", *Opt. Express* **2**, 483–490 (1998).
162. J. F. Henninot, M. Debailleul, R. Asquini, A. d'Alessandro, and M. Warenghem, "Self-waveguiding in an isotropic channel induced in dye doped nematic liquid-crystal and a bent self-waveguide", *J. Opt. A* **6**, 315–323 (2004).
163. F. Derrien, J. F. Henninot, M. Warenghem, and G. Abbate, "A thermal (2d+1) spatial optical soliton in a dye doped liquid-crystal", *J. Opt. A–Pure Appl. Opt.* **2**, 332–337 (2000).
164. S. V. Serak, N. V. Tabiryan, M. Peccianti, and G. Assanto, "Spatial soliton all-optical logic gates", *IEEE Photonics Technology Letters* **18**, 1287–1289 (2006).
165. A. Piccardi, A. Alberucci, U. Bortolozzo, S. Residori, and G. Assanto, "Readdressable interconnects with spatial soliton waveguides in liquid-crystal light valves", *IEEE Photon. Technol. Lett.* **22**, 694–696 (2010).
166. M. Peccianti and G. Assanto, "Signal readressing by steering of spatial solitons in bulk nematic liquid-crystals", *Opt. Lett.* **26**, 1690–1692 (2001).
167. J. Beeckman, K. Neyts, and M. Haelterman, "Patterned electrode steering of nematicons", *J. Opt. A* **8**, 214–220 (2006).

168. M. Peccianti, C. Conti, G. Assanto, A. De Luca, and C. Umeton, "All-optical switching and logic gating with spatial solitons in liquid-crystals", *Appl. Phys. Lett.* **81**, 3335–3337 (2002).
169. J. F. Henninot, J. F. Blach, and M. Warenghem, "Enhancement of dye fluorescence recovery in nematic liquid-crystals using a spatial optical soliton", *J. Appl. Phys.* **107**, 113111 (2010).
170. M. Peccianti, C. Conti, and G. Assanto, "Optical modulational instability in a nonlocal medium", *Phys. Rev. E* **68**, 025602 (2003).
171. J. Beeckman, K. Neyts, and M. Haelterman, "Induced modulation instability and recurrence in nonlocal nonlinear media", *J. Phys. B* **41**, 065402 (2008).
172. J. Beeckman, X. Hutsebaut, M. Haelterman, and K. Neyts, "Induced modulation instability and recurrence in nematic liquid-crystals", *Opt. Express* **15**, 11185–11195 (2007).
173. A. Fratalocchi, G. Assanto, K. A. Brzdakiewicz, and M. A. Karpierz, "Discrete light propagation and self-trapping in liquid-crystals", *Opt. Express* **13**, 1808–1815 (2005).

Biographies and photographs of the authors not available.